UNIVERSITAT POLITÈCNICA DE CATALUNYA
BARCELONATECH
Escola Superior d'Enginyeries Industrial,
Aeroespacial i Audiovisual de Terrassa

UNIVERSITAT POLITÈCNICA
DE CATALUNYA

MÀSTER UNIVERSITARI EN ENGINYERIA AERONÀUTICA

TREBALL FINAL DE MÀSTER

A study on Tensegrity Structure and their Applications to Space

Author:
Jamal OUBASLAM

Coordinators:
Juan Carlos CANTE,
David Roca CAZORLA,

June 22, 2021

Contents

List of Figures

List of Tables

Abstract

Tensegrity structures are pin-jointed truss structures compones of cables in tension and bars in compression. Due to their lightweight, complex shape topology and storage ability they can be a grate option for many application.

This project deals with computation method and analysis of tensegrity structures. The aim is to determine how this structures are developed in practice. To do so, different form-finding methods are used to determine a geometry without the necessity of knowing the nodal coordinates, just the connectivities between elements. This allows the user to find new shapes for this type of strutures.

As they are pre-stressed structures, it is important to determine their equilibrium position in absence of external forces. This process is called initial self-stress design. Once this initial state is known, it is possible to determine the structural behavior under external loads. For that reason, a non-linear Finite Element Analysis method for large displacements has been used to determine the response of the structure for a given structural load. This has been used then compare the pre-stressed structures to the normal pin-jointed structures by comparing the results of a linear method with the non-linea rone.

Finally, a small review about the possible applications of tensegrity structures for space applications is given. Specifically, the case of a two-stage tensegritic mast has been studied to give an idea about how these structures can be used for this purpose.

Resumen

Las estructuras de tensegridad son estructuras de articuladas con pasadores compuestas de cables en tensión y barras en compresión. Debido a su topología de forma compleja, peso, y su capacidad de almacenamiento, pueden ser una opción principal para muchas aplicaciones.

Este proyecto trata sobre el método de cálculo y el análisis de estructuras de tensegridad. El objetivo es determinar cómo se desarrollan estas estructuras en la práctica. Para ello, se utilizan diferentes métodos de búsqueda de formas para determinar una geometría sin la necesidad de conocer las coordenadas nodales, solo las conectividades entre elementos. Esto permite al usuario encontrar nuevas formas para este tipo de estructuras.

Al tratarse de estructuras pretensadas, es importante determinar su posición de equilibrio en ausencia de fuerzas externas. Este proceso se denomina diseño de autoesfuerzo inicial. Una vez conocido este estado inicial, es posible determinar el comportamiento estructural bajo cargas externas. Por esa razón, se ha utilizado un método de análisis de elementos finitos no lineal para grandes desplazamientos para determinar la respuesta de la estructura para una carga estructural determinada. Esto se ha utilizado para luego comparar las estructuras pretensadas con las estructuras normales unidas por pasadores comparando los resultados de un método lineal con el no lineal.

Finalmente, varias pinceladas sobre las posibles aplicaciones de estas estructuras en aplicaciones aeroespaciales son presentadas. Concreatemente, se ha estudiado el caso de un mástil tensegrítico de dos etapas para dar una idea de como estas estructuras se pueden usar para este fin.

Chapter 1

Introduction

Tensegrity structures have emerged as an architectural concept in the 1950s and nowadays they have many beneficial applications in science and engineering. This structures can be categorized as pre-stressed pin-jointed structures. They are composed of different material members or elements that can be bars or cables. The presence of pre-stress leads to cables in tension and bars in compression allowing the structure to be in self-equilibrium state. The concept of a self-stable structure is not new, but when the tensegrity concept is introduced, it becomes completely different.

The wide range of possibilities for geometrical design, lightness, material saving and great resistance that this structures offer, have made it easier to carry out varied and colorful works such as those made by the sculptor Kenneth Snelson.

On the other hand, deployable structures have emerged as a well option for easy storage and transportation. This idea has potential benefits both in Earth and in Space. For space application they are a need as the constant growing industry develop larger spacecrafts while the launch vehicles did in a different rate. For the future it is assumed that the launch vehicles capacity will remain unchanged while the need to launch larger spacecrafts (e.g *Next Generation Space Telescope* (NGST)) is constantly growing [30]. That is why tensegrity structures appear as a new way to design foldable structures for space applications.

Furthermore, tensegrities are suitable alternatives regarding conventional structures are suitable for the design of structural system with high complex topology and variable topological configurations [1]. Their structural modification (shape morphing) and adaptation might be easier for this type of structures. Other advantages of this structures from an engineering point of view, as already mentioned are: the mass efficiency, modularity, scalability, deployability and shape/stiffness flexibility.

In this project, the idea of tensegrity is structure is presented and a further research about this structures and the main ideas are explained such as the numerical computation of this structures and resolution.

The objectives of this project are:

1. Develop an algorithm for the form-finding of tensegrity structures. The form-finding is a key part for the design of this structures. This algorithm can be used for simple

and complex configuration by just knowing the desired shape (how bars and cables are connected).

2. Develop another method where some geometrical properties are know, not only connectivities and type of material. This involves also the development of a method to identify the initial self-stress state of a given structure, it there is some.

3. Investigation and test of the static properties of this type of structure under compression, traction and bending loads. Use this objective to compare them with the conventional pin-jointed truss structures and determine how pre-stress can help to improve the structural behavior.

4. Study of a possible application on space of this type of structure. A two stage mast will be studied under external loads and some data will be given regarding its deployability.

The present chapter contains a definition for tensegrity structures and their background. The actual applications of this structures are presented and their possible application into space environment is introduced.

1.1 Definition of Tensegrity Structures

The concept of tensegrity structure date back to the end of 1962s when Buckminster Fuller used the word *tensegrity* as a contracted form of *tensile* and *integrity* to Kenneth Snelson‘s structure [8]. Fuller describes a tensegrity structure as

“an assemblage of tension and compression components arranged in a discontinuous compression system...”

while Hanaor [11] gives a more specific definition which is

“internally pres-tressed, free-standing pin-jointed networks, in which the cables or tendons are tensioned against a system of bars or struts”

The mechanical principle of this structures can be deduced to be a set of cables in traction and bars in compression interconnected to generate self-stressed structure. Tensegrity structures are pre-stressed structures and then they are obtained from an optimal arrangement of materials, which must be in tension or compression. They consist of two components or structural elements, namely the tensile and compressive members, which are cables (or strings) and bars (or struts) respectively.

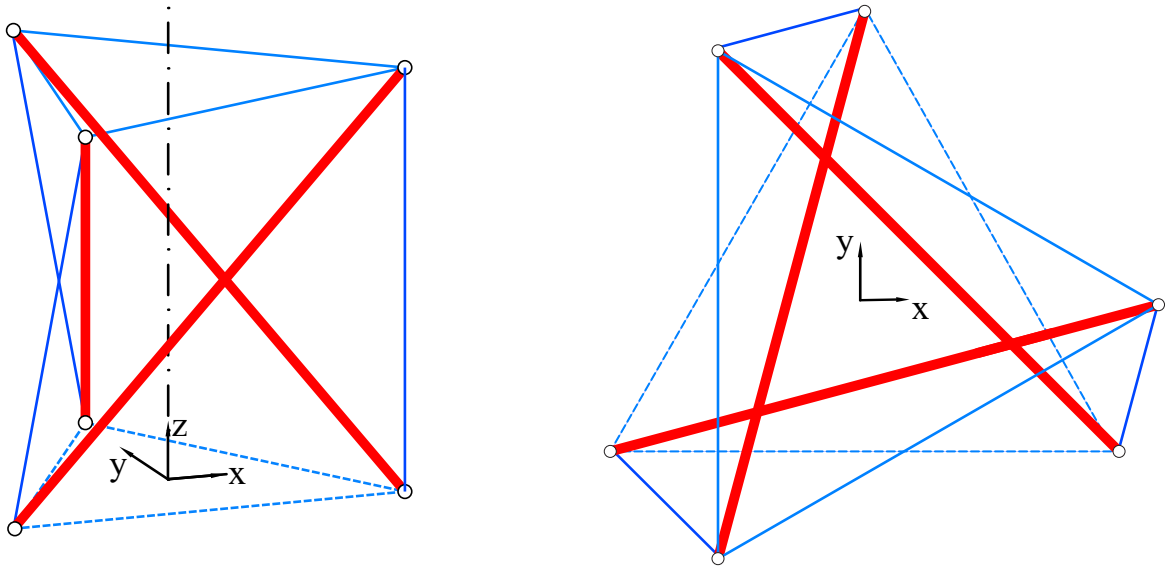

FIGURE 1.1: Tensegrity structure with 3 bars (red) and 9 cables (blue). Side view in left side and top view at the right side.

Fig. 1.1 shows a simple tensegrity structure and it is noticeable that the bars does not touch between them and they are not connected through the *nodes* while the cables are interconnected at every node forming a network. That is why traditionally tensegrity structures are described as *"islands of compression inside an ocean of tension"* [15]. In a pure tensegrity (Class I), which is the case shown in Fig. 1.1, the structure is defined by a set of independent elements which are connected through nodes (as pin-jointed structures). This excludes conventional structures and those ones with cables but with connected bars. A more specific definition to tensegrity structure is defined as systems *"whose rigidity is the result of a state of self-stress equilibrium between cables under tension and compression elements and independent of all fields of action"* [18].

Additionally, since the bars can be considered as inelastic rigid bodies, the structural system is only stabilized by the presence of internal tension through the cables (inducing a compression in bars) and in the absence of external forces [27]. This means that the structural system must remain in equilibrium although no external loads are acting on it. If a small perturbation is introduced to system, it must return to its initial state.

There are also tensegrity structures where the bars are interconnected, but they are called *false* tensegrities or Class II tgensegrities. However, there are cases where this type of tensegrities can be of great interest as we will see in later chapters.

1.2 Research and Application

The sculptors, artists, and architects have long been fascinated by the magnificence of tensegrity structures ever since their appearance and notoriety. In art, tensegrity structures are of high interest due to their aesthetic value. They have been used to create unique geometrical arrangements of bars and cables with striking beauty and complex configurations [9]. This system is not only used as an artistic expression, great referents in the structural field(civil engineering,architecture,etc) have promoted the use of tensegrity in the last decades. Among others, the Georgia Dome inaugurated in 1992 is one of the

most important although not being a pure tensegrity as the dome is anchored to a concrete ring. Another example is the Kurilpa Bridge in Australia, which is considered the longest tensegritic pedestrian bridge in the world. It was inaugurated in 2009 over the Brisbane River.

The concept of tensegrity is also present in some areas such as science (e.g-structure of spider fibre) and, in man and many types of animals, bones (rigid bodies) and tendons (elastic bodies) are connected together and can be moved from one equilibrium position to another by only tensile forces in tendons. That is why in osteology different configurations are classified as different tensegrity structures [27].

In mechanical engineering, the concept of tensegrity has been used for the manufacturing of furniture, robots [25], electrical transducers [4], among others. From an engineering perspective, tensegrities are ideal candidates for deployable structures as they can undergo large displacements and be very lightweight. With the development of numerical models and folding process[9], the use of tensegrity as deployable structures opened up significantly. This deployability has been of important interest in space industry. The actual applications of tensegrity structures in space application are treated in the following section.

1.3 Deployable Structures for Space Applications

One of the biggest problems when dealing with space missions is the storage capability for the given payloads, restricting their weight and volume. A solution to that problem in common situations is the use of devices which configuration changes from a packaged, compact state to a deployed, large state [30]. Deployable structures have been used widely in space applications and missions for several decades due to their easy storage and transportation.

Several research has been done over the past five decades in the field of deployable space structures. Among the existing concepts: some structures can be retracted after they are deployed, other relay on stored strain energy for deployment, and some structures are stiff during deployment. The retraction of the structure in space is not a direct necessity, but may be required in some cases[30]. The structures that are not dependent of stored energy are deployed through external tools (e.g. motor, actuator). Normally, deployable structures are not stiff during deployment but some other can immediately carry loads.

Actually, there are three types of devices where the structure deployability concept is present.

- **Masts**: they are normally used to separate electronic instruments to reduce interference[17] or to support solar arrays[13].
- **Antennas**: the need of communication with orbiting objects (satellites) provokes the need of some antenna. Among the different set of antennas, the parabolic reflector antennas are the most common used due to their high gain, enabling high data transmission at low power [30].
- **Solar Panels**: The actual capacity of the solar arrays is not enough for increasing electrical needs of actual satellites. That is why some system to pack the solar arrays

in launcvh and deploy them in space is required.

Both deployable antennas and solar panels are not in the outline of this project and they will not be reviewed. However, deployable antennas are studied in detail by Tibert and Pellegrino [29, 30] and their relation to tensegrity. Also there are a lot of deployable masts that will not be commented, but a further explanation can be found in [17].

Deployable Masts

According to [17], deployable masts can be divided into the following four groups:

1. Thin-walled tubular booms,
2. Teslescopic masts,
3. Coilable masts, and
4. Articulated trusses

1- Thin-walled tubular booms

Thin-walled tubular booms are considered the earliest types of deployable and retractable structures. Their principle of work is by taking advantage of the elastic deformability of thin-walled cells.

The first thin-walled tubulars are the *Storable Tubular Extendible Member* (STEM), invented in Canada in the 1960s. This systems were stiff axially and in bending, but they had low torsional stiffness due to the open tubular cross-section. This lack in torsional stiffness can be solved if enough friction is produced in the overlap region [30]. The Collapsible Tubular Mast (CTM) is the composition of two STEM bonded at the edges, providing higher torsional stiffness. CTMs where developed by the German Aerospace Centre (DLR) and they are made of Carbon Fibre Reinforced Plastic (CFRP).

2- Telescopic Masts

This type of mast is normally composed by a series of thin-walled cylindrical tubes nested one inside another. Their limiting factor resides in the tube thickness and overlap length.
This mast are deployed through a spindle-and-nut technique (sequential deployment), or adding cables and pulleys (synchronous deployment) as shown in Fig. 1.3. *Dornier* [14] and Tethered Satellite [20] have developed a 40 m and a 2.4 m long telescopic masts respectively.

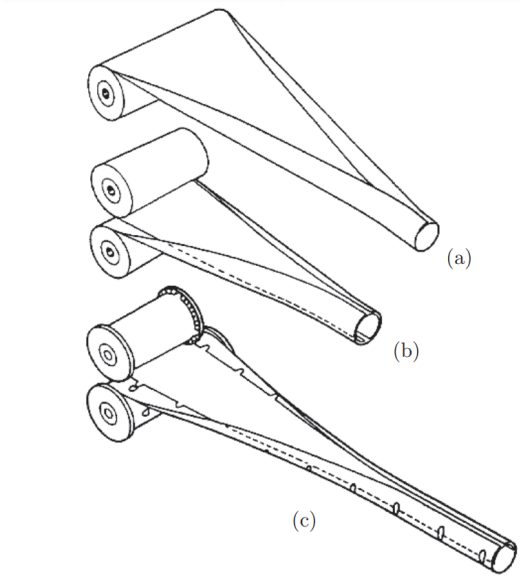

(A) STEM booms: (a) STEM, (b) bi-STEM, and (c) interlocking bi-STEM [30]

(B) Collapsible Tubular Mast [16]

FIGURE 1.2: STEM and CTM thin-walled tubular booms[30]

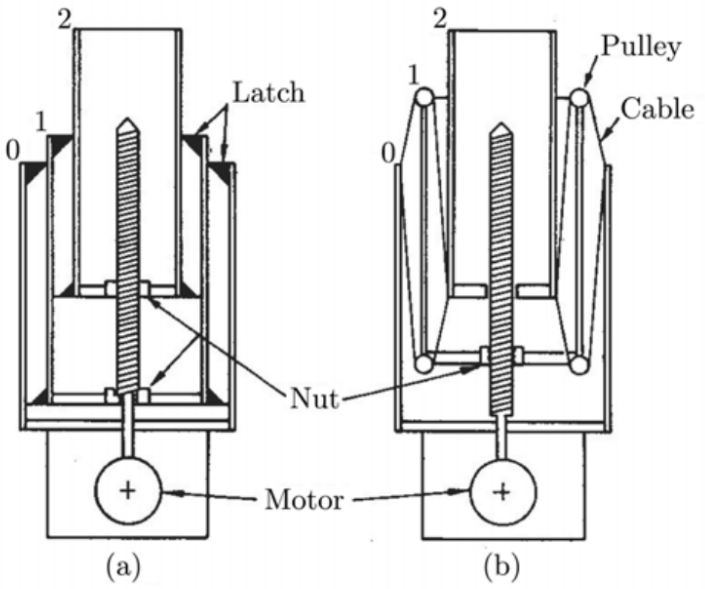

FIGURE 1.3: Telescopic masts deployment techniques: (a) sequential and (b) synchronous

As it can be seen from Fig. 1.3, a motor drives the spindle and in each stage there is a nut which is dragged outward until reaching the spindle height.

3- Coilable Masts

In 1967, the *Astro Research Corporation* developed the *Coilable Mast* (CM). Thi type of mast is a lattice truss that normally consist of three types of elements, called battens,

longerons and bracing cables. The connection between elements consists of members perpendicular to the longitudinal ones and diagonal cables [30]. Coiling the longerons is the way in which this mast is stowed. They are design in a way that the lateral battens always carry compression, and inducing pre-stress in the structure.

Coilable masts can be deployed through two ways:

- **Self driven extension**: this method uses the stored elastic energy in the longerons. The rate of deployment is controlled through a lanyard (i.e. using a cable attached to the top of the mast in order to control the deployment and retraction). The stiffness of the mast is lower during deployment than when deployed, and then it is not suitable for masts longer than 3 m.
- **Motor driven extension**: this method is used for longer masts and, as in Fig. 4.11, the mast is confined in a special canister (which contains a motor driven rotating nut). The transition where a stage goes from stowed to deployed is inside the canister ensuring full strength to the deployed part.

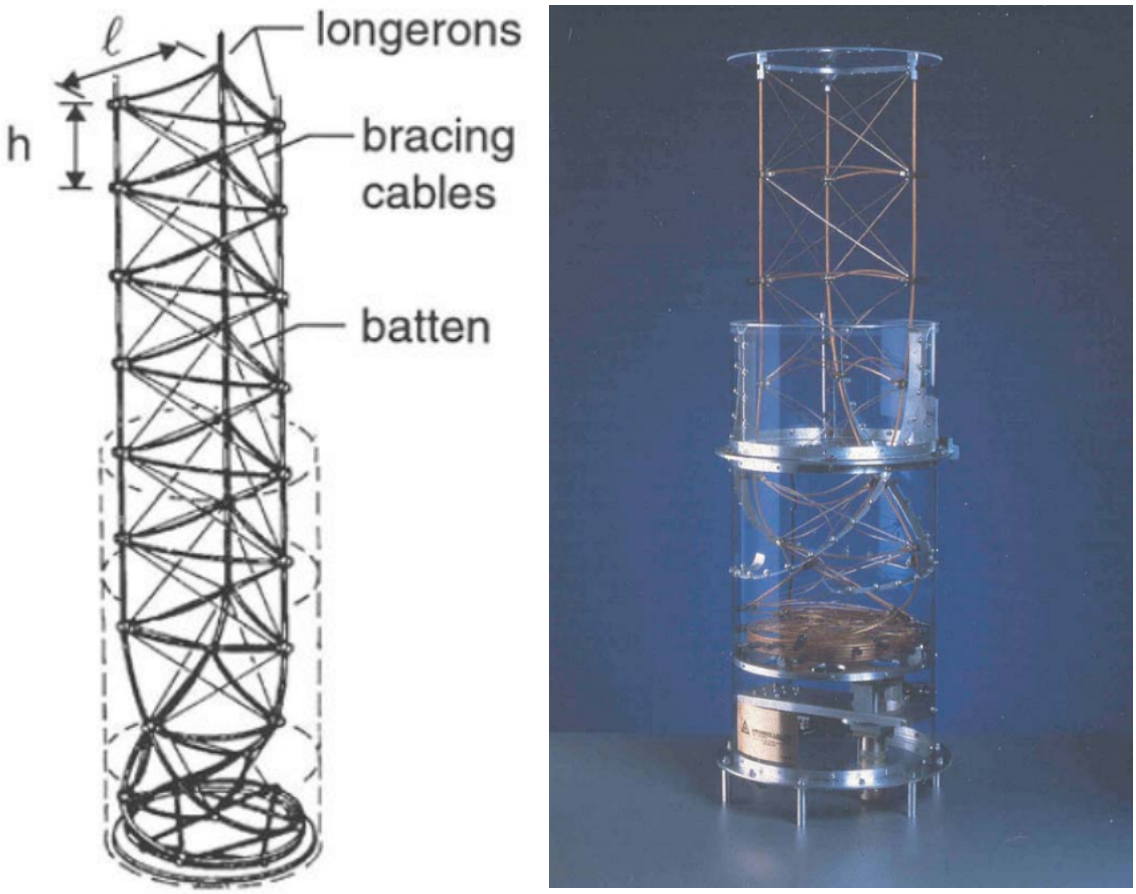

FIGURE 1.4: Coilable mast concept (left) [34] and application inside a canister and deployed through a rotating nut (right) [30]

The coilable masts are really efficient in terms of packing or stowage as they can be stowed about 2–3% of the deployed length.

4-Articulated Trusses

Articulated trusses are types of masts widely used for space applications and can be found in different configurations. They present higher stiffness than the other types of deployable masts as long as a better structural efficiency. The *Folding Articulated Square Truss* (FAST) mast, developed by AEC-Able Engineering Company is an example of this type of structure. It is composed by revolute hinges along the longerons and two pairs of diagonal cables at each face of the bay, Fig. 1.5. The cables are supposed to be pre-stressed through two lateral bows.

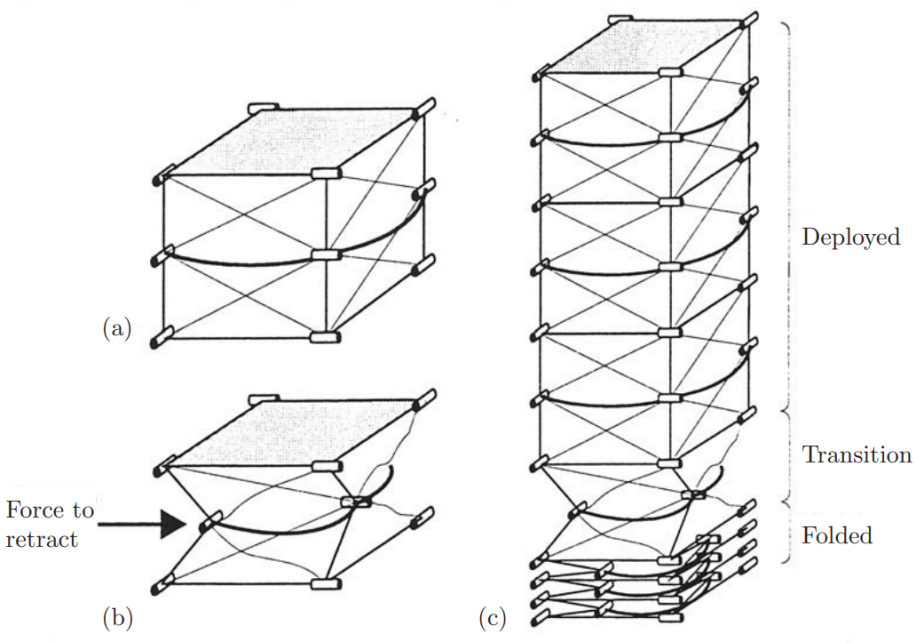

FIGURE 1.5: Folding Articulated Square Truss deployment description [29]

FIGURE 1.6: FAST mast for the ISS [30]

During deployment process, as the bows bend, half of the cables become slack and the strain energy stored in the bows deploys one bay of the mast (see Fig. 1.5(b,c)). As for the CMs part of the mast is enclosed in a special canister, ensuring the total stiffness of the deployed part of the mast. Two FAST masts, of 1.09 m diameter and 34.75 m length are used to support the solar arrays on the *International Space Station* (ISS), Fig. 1.6

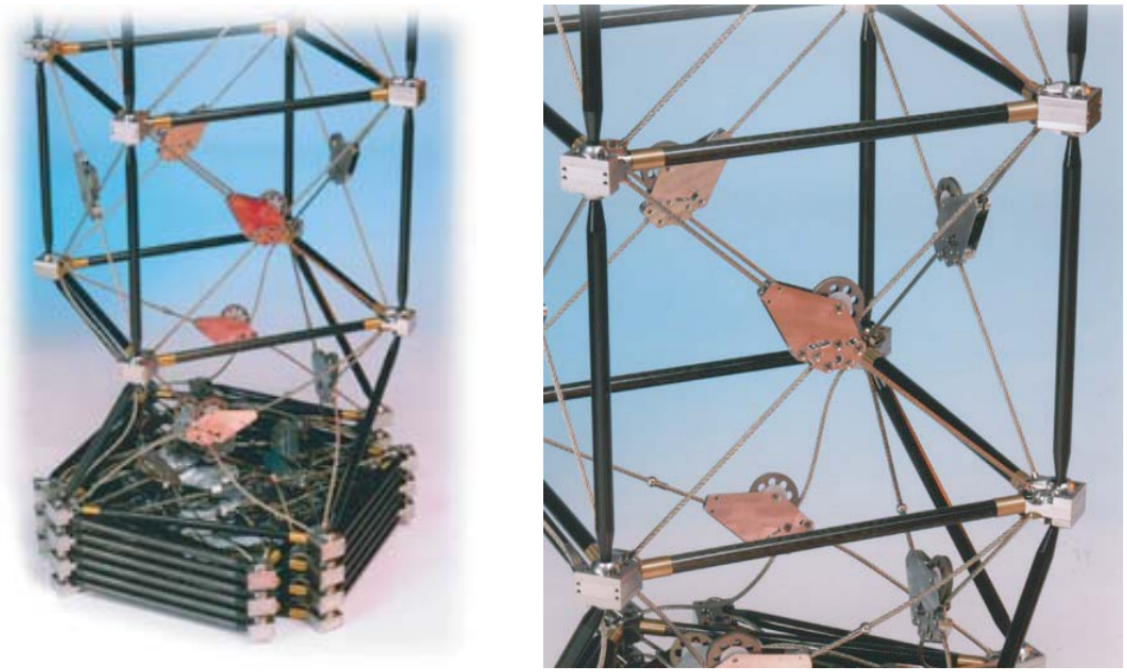

(a) (b)

FIGURE 1.7: Deployment of ADAM mast [30]

Another notorious example of articulated truss mast is the *Able Deployable Articulated Mast* (ADAM) as it has used in the *Shuttle Radar Topography Mission* (STRM), an Earth mapper. The main function of this mast is to separate two radar antennas. The STRM ADAM is 60 m long and has a diameter of 1.12 m and 87 bays. The deployment sequence is shown in Fig. 1.7 and it can be noticed that some special latches are used on the diagonal cables in order to stop the deployment and stiff the corresponding bay.

Now that tensegrity structures are introduced and their applications are presented, it is time to start studying the mathematical development of this type of structures.

Chapter 2

Mechanics and Analysis Methods of Tensegrity Structures

A tensegrity structure follows the same fundamental idea as any conventional pin-jointed structure: the condition of static equilibrium exist if the net sum of forces acting at any point of the structure must be zero. This leads to a governing equation where the internal forces compensate the external loads. Tensegrity structures are composed of truss elements and this condition must be applied at the end of each element, called node.

The initial issue when dealing with the design of tensegrity structure, as for any other structure, is to determine the optimal structural form, the form-finding process. The majority of the research done in the field of tensegrity structures is dedicated to the form-finding process.

In this chapter the equilibrium equations for a tensegrity structure are presented and two different methods used to determine the form-finding of tensegrity structure are presented.

2.1 Equilibrium Equations

Imagine that there are 3 nodes in a 3-dimensional space, called j, k and h, connected to another node i through a structural element that may only experience axial force. This situation can be directly interpreted as an element of a tensegrity structure and that the nodes are connected through elements such as cables or bars. 2.1 show the situation described above where the force in red f is an external force applied over the node i.

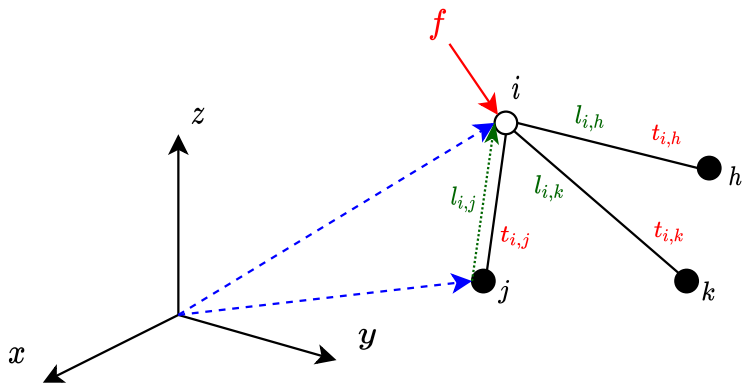

FIGURE 2.1: Node i connected to nodes j, k and h and over an external force f

The following assumptions are made in order to determine the equilibrium equations:

- The members are connected through ideal ball joints.
- The weight of the structure is neglected.
- The external forces act directly at the nodes.
- The connectivity of the system are known.

The equilibrium in Node i is given by the condition that the internal forces from the three jointed members or elements balance with the applied external forces.

$$\vec{t_{i,j}} + \vec{t_{i,k}} + \vec{t_{i,h}} + \vec{f} = \vec{0} \tag{2.1}$$

where $\vec{t}$ denotes each member force or internal tension, also known as pre-stress force vector. If the coordinates of each node are known the vectors pointing from one point to another can be easily computed. With this the direction of the internal forces can be found but not the magnitude. This can be solved normalizing this vector by the current member length in order to have a unity vector along each member that can be then multiplied by a parameter representing the internal force magnitude [7]. An example for the internal force coordinate representation of the member ij

$$\{t_{j,i}\} = \frac{t_{i,j}}{l_{i,j}} \begin{Bmatrix} x_i - x_j \\ y_i - y_j \\ z_i - z_j \end{Bmatrix} \tag{2.2}$$

where $t_{i,j}$ is the magnitude of the internal force, $l_{i,j}$ the element length and x,y and z the coordinates of both element nodes. Then, the equilibrium equations for the Node i is:

$$\frac{t_{i,j}}{l_{i,j}} \begin{Bmatrix} x_i - x_j \\ y_i - y_j \\ z_i - z_j \end{Bmatrix} + \frac{t_{i,k}}{l_{i,k}} \begin{Bmatrix} x_i - x_k \\ y_i - y_k \\ z_i - z_k \end{Bmatrix} + \frac{t_{i,h}}{l_{i,h}} \begin{Bmatrix} x_i - x_h \\ y_i - y_h \\ z_i - z_h \end{Bmatrix} + \begin{Bmatrix} f_x \\ f_y \\ f_z \end{Bmatrix} = \begin{Bmatrix} 0 \\ 0 \\ 0 \end{Bmatrix} \tag{2.3}$$

Note that in order to be the members in tension the internal force magnitude must be negative by convention (positive for compression and negative for tension). This will only change the current direction to the opposite one. Rearranging terms the above system of equations can be expressed in matrix form as:

$$\begin{bmatrix} x_i - x_j & x_i - x_h & x_i - x_k \\ y_i - y_j & y_i - y_h & y_i - y_k \\ z_i - z_j & z_i - z_h & z_i - z_k \end{bmatrix} \begin{Bmatrix} \frac{t_{i,j}}{l_{i,j}} \\ \frac{t_{i,h}}{l_{i,h}} \\ \frac{t_{i,k}}{l_{i,k}} \end{Bmatrix} = \begin{Bmatrix} f_x \\ f_y \\ f_z \end{Bmatrix} \tag{2.4}$$

Note that the variable $t_{i,n}/l_{i,n}$ denotes the internal force carried by each member per unit length, which is the definition of **force density** or tension coefficient. Regarding the first term of the equation one can deduce that the columns of the matrix correspond to a member while the rows are the conditions for nodal equilibrium in different directions. For a given node there must be d rows, being d the space dimension. If this equilibrium equations are written for each node the equilibrium equation of the whole structure can be found. In a generalized form, given a structure with n nodes and b elements, the matrix will take an

order of dn rows and b columns. If a member m connects node i and j, in the mth column only $2d$ rows corresponding to node i and j projections are to be filled in, while all the other entries are set to 0. For an extended structure Eq. (2.4) becomes:

$$\begin{bmatrix} \cdots & 0 & \cdots \\ \cdots & \vdots & \cdots \\ \cdots & x_i - x_j & \cdots \\ \cdots & y_i - y_j & \cdots \\ \cdots & z_i - z_j & \cdots \\ \cdots & 0 & \cdots \\ \cdots & \vdots & \cdots \\ \cdots & -\left(x_i - x_j\right) & \cdots \\ \cdots & -\left(y_i - y_j\right) & \cdots \\ \cdots & -\left(z_i - z_j\right) & \cdots \\ \cdots & 0 & \cdots \\ \cdots & \vdots & \cdots \end{bmatrix} \begin{Bmatrix} \vdots \\ q_{i,j} \\ \vdots \end{Bmatrix} = \begin{Bmatrix} \vdots \\ f_{i,x} \\ f_{i,y} \\ f_{i,z} \\ \vdots \end{Bmatrix} \tag{2.5}$$

In compact vector-matrix form the system becomes:

$$\mathbf{Aq} = \mathbf{f} \tag{2.6}$$

Where $[\mathbf{A}] \in \mathbb{R}^{dn \times b}$ is known as **equilibrium matrix**, $\{\mathbf{q}\} \in \mathbb{R}^{b}$ the force density vector and $\{\mathbf{f}\} \in \mathbb{R}^{dn}$ the vector of external forces [7].

To represent the equilibrium equations a connectivity matrix defining the topology of the tensegrity structure can be used [23, 19, 32]. This matrix $[\mathbf{C}] \in \mathbb{R}^{n \times b}$ has many columns as nodes and many rows as elements. If element k connects node i and j the entry of ith node-column takes a value of $+1$ while the jth column takes the value of -1.

$$\mathbf{C}_{(k,p)} = \begin{cases} 1 & \text{if } p = i \\ -1 & \text{if } p = j \\ 0 & \text{if otherwise} \end{cases} \tag{2.7}$$

Assuming that **x**,**y** and **z** are the nodal coordinate vectors of a given structure, the equilibrium matrix $\mathbb{A}$ can be written as:

$$\mathbf{A} = \begin{bmatrix} \mathbf{C}^T \operatorname{diag}(\mathbf{Cx}) \\ \mathbf{C}^T \operatorname{diag}(\mathbf{Cy}) \\ \mathbf{C}^T \operatorname{diag}(\mathbf{Cz}) \end{bmatrix} \tag{2.8}$$

The equilibrium equation in Eq. (2.33) can be expressed in an alternative form just rearranging the terms in a different manner. Scheck [23] gave the following relationship for any general pin-jointed structure:

$$\mathbf{D}\,[\mathbf{x}\ \mathbf{y}\ \mathbf{z}] = [\mathbf{f_x}\ \mathbf{f_y}\ \mathbf{f_z}] \tag{2.9}$$

The matrix $[\mathbf{D}] \in \mathbb{R}^{b \times b}$ is also called force-density matrix [2, 29] and with a known connectivity matrix is can be expressed as follows through the Gaussian transformation

$$\mathbf{D} = \mathbf{C}^{\mathrm{T}}\mathbf{QC} \tag{2.10}$$

where $[\mathbf{Q}] \in \mathbb{R}^{b\times b}$ is a diagonal matrix containing the members force densities.

$$\mathbf{Q} = diag\,(\mathbf{q}) \tag{2.11}$$

And elements of the force-density matrix $\mathbf{D}$ interpretation is [10]:

$$D(i,j) = \left\{ \begin{array}{ll} -q_b & \text{if member } b \text{ is connected with nodes } i \neq j, \\ \sum q_b & \text{sum up for all members } b \text{ connected to nodes } i \\ & \text{when } i = j, \\ 0 & \text{if nodes } i \text{ and } j \text{ are not connected} \end{array} \right\} \tag{2.12}$$

As a tensegrity structure has to remain in static equilibrium in absence of external loads, the equilibrium condition becomes:

$$\mathbf{Aq} = \mathbf{0} \tag{2.13}$$

and consequently

$$\mathbf{D}\,[\mathbf{x}\ \mathbf{y}\ \mathbf{z}] = [\mathbf{0}\ \mathbf{0}\ \mathbf{0}] \tag{2.14}$$

Note that both expressions in Eq. (2.13) and Eq. (2.14) are the same but with different representation. The first one represents the self-equilibrium equations as a function of the nodal coordinates, while the second one does in terms of the element force densities. Even they are the same, both must be fulfilled for a tensegrity structure in order to be in self-equilibrium state in absence of external forces.

Note that a trivial solution becomes as the first solution for this scenario. Nevertheless this does not match with the definition of tensegrity as the cables need a pre-stress to be taut and the structure remains in equilibrium (for a structure to exist in a real physical space, $\mathbf{q}$, cannot be zero). That is why in order to satisfy the condition of equilibrium under self-stress conditions, $\mathbf{A}$ has to be singular. As no kinematic considerations are made, the shape of the matrix normally has more rows than rows, being rectangular and not square. Then it is also necessary that the matrix $\mathbf{A}$ has no full column rank. As the matrix is rank deficient this matrix cannot be generated randomly. Even if a matrix with this conditions is obtained, the force densities $\mathbf{q}$ for each element can only be chosen from its null space.

Another interpretation that can be given to the previous equation is that the shape of the structure, described by the equilibrium matrix, is not arbitrary (desire nodal coordinates). Then it is necessary to find a particular shape for the structure in order to satisfy the initially defined connectivity (nodal coordinates). Solving this system is what it is called form-finding process.

2.1.1 Rank Conditions

As mentioned before, for a d-dimensional structure that is a state of self-stress two but not sufficient rank conditions must be satisfied [2, 19, 5]. They are directly related to the equilibrium and the force-density matrices where the solution(nodal coordinates and internal force-densities) for the self-stressed tensegrity are obtained. The first rank deficiency conditions ensures at least one state of self-stress for the given structure if

$$r_A = rank(\mathbf{A}) < b \tag{2.15}$$

which is necessary for a non-trivial solution of the Eq. (2.13) to be found from the null-space of the equilibrium matrix. In previous expressions, b represent the number of members or elements.

The second rank conditions is related to the semi-definite matrix $\mathbf{D}$ as follows for a geometric embedding in $\mathbb{R}^d$:

$$r_D = rank(\mathbf{D}) < n - d \tag{2.16}$$

where d is the space dimension and n the number of nodes. With this condition, d-particular solutions for Eq. (2.14) exist generating a d-dimensional structure [34]. For an embedding of maximal affine space [5] the largest possible rank of $\mathbf{D}$ is $(n-d-1)$. This means that the matrix has a nullity of $(d+1)$.

2.1.2 Static and Kinematic Indeterminacy

A structure is said to be in statically and kinematically determinate when the equilibrium equations are sufficient to determine the internal forces in the elements (number of eq. equations is equal to number of unknown forces). Otherwise, if some additional structural members than the ones strictly needed are added, additional stresses will be internally introduced in general. Since there are more unknowns than then ones than can be obtained from the equilibrium equations, more than one solution for the internal tensions in members will be obtained. The structural system then becomes statically indeterminate and the structure is said to be in a sate of self-stress.

On the other hand, if some element is removed from the structural system, the structure geometry cannot be specifically determined and a set of independent infinitesimal mechanics appear in the assembly [1, 24]. The system is then said to be kinematically indeterminate. The introduction of infinitesimal mechanisms means that the nodes of the structure can move infinitesimally without changing the member lengths.
The static and kinematic determinacy is directly governed by the generalized Maxwell's rule

$$dn - b - r_{bm} = m - s \tag{2.17}$$

were r_{bm} is the number rigid body motions. If s or m is determined, the Maxwell's rule can be used to compute the other one. However, with the first rank condition explained before, the number of structural independent states of self stress and the number of infinitesimal mechanisms can be obtained from the equilibrium matrix rank r_A as studied by Calladine in its investigation for a generalized Maxwell's rule for tensegrity structures [3].

$$s = b - r_A \leq 1 \tag{2.18}$$

$$m = dn - r_A \tag{2.19}$$

Through this two parameters, pin-jointed structures can be classified as follows [3, 22]:

Assembly Type	Condition	Static and Kinematic Properties
I	$s = 0$ $m = 0$	Statically determinate and Kinematiically determinate
II	$s = 0$ $m > 0$	Statically determinate and Kinematiically indeterminate
III	$s > 0$ $m = 0$	Statically indeterminate and Kinematiically determinate
IV	$s > 0$ $m > 0$	Statically indeterminate and Kinematiically indeterminate

TABLE 2.1: Classification of structural systems

The group of tensegrity structures is the 4th one as they present static indeterminacy for self-equilibrium theory. On the other hand, they normally are kinematically indeterminate thus reducing the overall stiffness of the structure due to infinitesimal mechanisms [34]. Then the initial configuration is not unique but one can still set up an initial configuration to obtain the equilibrium matrix by assuming that small-deflection theory [1].

2.1.3 Physical Interpretation of the SVD

Similar to other assemblies, a wealth of information can be obtained from the four fundamental spaces (the row space, column space and left null space) of the equilibrium matrix **A**. This spaces are obtained from the factorization of the equilibrium matrix through a Single Value Decomposition as shown in Fig. 2.2 [22, 21]. Then, SVD is a factorization of a positive semidefinite matrix (e.g a symmetric matrix with positive eigenvalues) to any $m \times m$ through and extension of the polar decomposition. That is why is useful for electrical applications and structural mechanics. The SVD decomposition for the equilibrium matrix **A** is given as follows:

$$\mathbf{A}_{m\times n} = \mathbf{U}_{m\times m}\Sigma_{m\times n}\mathbf{V}^T_{n\times n} \tag{2.20}$$

where $\mathbf{U} \in \mathbb{R}^{m\times m}$ is a real unitary matrix, $\Sigma \in \mathbf{R}^{m\times n}$ a rectangular matrix with positive real numbers in its diagonal, and $\mathbf{V} \in \mathbb{R}^{n\times n}$ is a real unitary matrix. The entries in the diagonal of Σ, called σ_{ii} in Fig. 2.2, are called the singular values of **A**. The columns of **U** and the columns of Σ are called the left-singular vectors and the right-singular vectors of **A**, respectively.

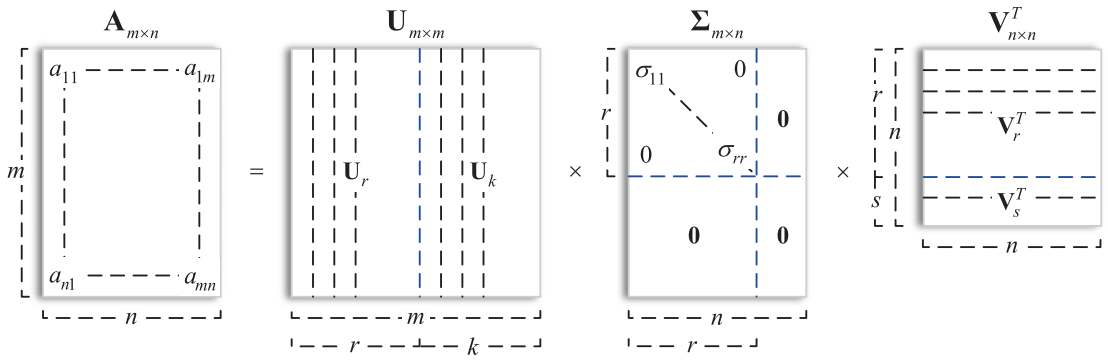

FIGURE 2.2: Singular value decomposition of the equilibrium matrix. Relationship between m, s, r and the matrix decomposition $\mathbb{U}$, Σ and $\mathbb{V}$ [1]

For a given matrix $\mathbf{A} \in \mathbb{R}^{m\times n}$, with rank r, the caracteristics from the SVD decomposition are the following:

- Matrix $\mathbf{U} \in \mathbb{R}^{m\times m}$ shows orthonormality as $U^T\mathbf{U} = I$ (where I is the identity matrix) as each column or row are orthogonal unit vectors ($u_{j=1,m}$).
- Matrix $\Sigma \in \mathbb{R}^{m\times n}$ has positive non-zero singular values σ_{ii} in its diagonal.
- Matrix $\mathbf{V}^T \in \mathbb{R}^{n\times n}$ is orthonormal $V^T\mathbf{V} = I$ and each row vector $v_{j=1,n}$ of matrix $\mathbf{V}$ is orthonomal.

The SVD decomposition is presented here as it will be the basis to get the solution to initial pre-stress from the null-space of the equilibrium matrix $\mathbf{A}$.

2.2 Form-Finding

One of the most critical parts in the design of a tensegrity structure is the form finding one. As mentioned in previous sections, the form-finding requires a solution for Eq. (2.13) and Eq. (2.14) (which means that a geometry shape and force-density at each element is found) under the rank deficiency conditions.

Form-finding methods for tensegrity structures have been studied along the years and some remarks are given to the work done by Conelly and Terrell [6], Vassart and Motro [33] and Sultan *et al.* [28]. In this section the actual existing methods for form-finding are classified as done by Tibert in [30] as: static and kinematic form-finding (FF) methods. A summary of each one of them is given but they will not be explained in further detail as just two one of them will be used.

- **Kinematic FF methods**: for this methods, the lengths of the cables are kept constant while the struts length is increased until reaching a maximum. Same procedure can be done keeping constant strut length and changing the cable ones until reaching a minimum. Note that this ensures cables in tension and struts in compression which mimics the way in which tensegrities are built in practice, without requiring explicitly a pre-stress in cables [30]. This methods can be solved through:

  - Analytical Solutions
  - Non-Linear Programming
  - Dynamic Relaxation

- **Static FF Methods**: this methods are characterized by the set up relation between equilibrium configurations of a structure with given topology and the member forces. Various methods can be used for this analysis such as:

  - Analytical Solutions
  - **Force-density Method**
  - **Reduced Coordinates**
  - Energy Method

An extensive explanation of this methods can be found in the work done by Tibert and Pellegrino [29, 30]. In this study, the force density method is implemented due to its intuitive implementation and straight forwardness. Also the reduced coordinates method is used to determine the nodal locations of a two tensegrity mast, which will be explained in later sections.

The force density method for cable structures was first proposed by Linkwitz and Scheck [23], where a simple mathematical trick is used to transform the non-linear equilibrium equations of each node into a set of linear equations. This has been previously explained but it is recalled now. For example, the equilibrium equation of a node i in the x direction is

$$\sum_j \frac{t_{ij}}{l_{ij}} \left(x_i - x_j\right) = f_{ix} \tag{2.21}$$

where node i is connected to no de j through a cable or a strut and t_{ij} is the tension in the element (or member). Although the equations seems to be linear, the length of the element l_{ij} also depend on the nodal coordinates. That is why the previous expression can be normalized for the element for-density as

$$q_{ij} = t_{ij}/l_{ij} \tag{2.22}$$

whose value needs to be known (or approximated) at the beginning of the form-finding. In the following section will deal with the implementation of this method to determine super-stable tensegrities with positive semi-definite matrix $\mathbf{D}$ with nullity $d+1$. Vassart and Motro [33] list three ways to determine a set of force-densities that achieve the required nullity: (i) intuitive, (ii) iterative and (iii) analytical [30].

From the previous three techniques, the first one is valid for a few element number; the second one is based in a trial and error research of nodal coordinates and force-density vector from the nullity of $\mathbf{A}$ and $\mathbf{D}$; and the third analysis $\mathbf{D}$ in a symbolic or semi-symbolic form. The second and the latter one are most effective ones and they are studied for a simple example of tensegrity.

2.2.1 Numerical Force-Density Method

This method was extensively studied by Estrada *et all* in [2] and contrary to most existing form-finding procedures [19, 29], a method where no initial assumptions about the elements lengths, geometry or symmetry of the structure are not required (but they can be as we will see later). The unique requirement for this method is that the connectivity between elements and element type are intuitively set up, use a predefined even number of nodes and a prototype of force density vector.

The prototype force-density vector is selected to be 1 for elements in tension and -1 for elements in compression, such that:

$$\mathbf{q}_0 = [\underbrace{+1+1 \quad +1}_{\text{tension}} \cdots \underbrace{-1-1}_{\text{compression}} \ ]^T \tag{2.23}$$

Then, the force-density matrix $\mathbf{D}$ is calculated using Eq. (2.10) and iteratively changed until the rank condition Eq. (2.16) is satisfied. It is important that during the iteration process the signs of the prototype force-density vector remain unchanged. Now the coordinates of the structure can be approximate from the eigenvalue or Schur decomposition of D expressed by:

$$\mathbf{D} = \mathbf{W}\mathbf{Y}\mathbf{W}^T \tag{2.24}$$

If matrix $\mathbf{D}$ has maximal rank, i.e, $rank(\mathbf{D}) = n - d - 1$, the first $(d+1)$ of the unitary matrix $\mathbf{W} = [w_1\ w_2\ w_3\ ...\ w_n]$ contains the basis of the nodal coordinates which solve the homogeneous equation Eq. (2.14). The diagonal matrix $\mathbf{Y}$ has $(d+1)$ zero eigenvalues. The nodal coordinates then can only be approximated for and arbitrary q. That is why the force-density matrix $\mathbf{D}$ corresponding to the prototype $\mathbf{q_0}$ is not unlikely to satisfy the rank requirement and therefore the structure is not in self-equilibrium. With this in mind, an approximate set of eigenvector columns that satisfy the equilibrium condition Eq. (2.14) is required.

An eigenvector column will be candidate for nodal coordinate if none of the members has zero length but as short as possible. Considering the problems in terms of length it is possible to choose an appropriate set of coordinates $\{w_i, w_j, w_k\}$ in which the total square length of the entire structure is minimized:

$$\sum_{e=1}^{b} l_e^2 = \left\| C\mathbf{w}_i + C\mathbf{w}_j + C\mathbf{w}_k \right\|^2 \tag{2.25}$$

To do so, the matrix $\mathbf{W}$ and the connectivity know matrix $\mathbf{C}$ are used to determine the projected lengths

$$\mathbf{L} = \mathbf{C}\mathbf{W} = \left[\left(\mathbf{w}_1^A - \mathbf{w}_1^B \right) \left(\mathbf{w}_2^A - \mathbf{w}_2^B \right) \cdots \left(\mathbf{w}_\mathrm{n}^A - \mathbf{w}_\mathrm{n}^B \right) \right] \tag{2.26}$$

along all n directions for each pair $(A.B)$ of connected nodes. The column vector w_i for which $Cw_i = 0$ can be removed. Now to identify the set $\{w_i, w_j, w_k\}$ for Eq. (2.25), the columns of $\mathbf{L}$ are identify by their 2-norm [2]

$$\left[\ c_1\ c_2 \quad \cdots \ \right] = \underset{i}{arg\,min} \, \|L_i\| \tag{2.27}$$

where the coefficients $c_1, c_2, ...$ returned by this minimal argument function are the indices in which the norm vector $\|L_i\|$ is minimized. The minimal indices are then taken as also their multiplicity to have a pool of at least d candidate columns. The search of candidates can be more narrowed up if the reduced matrix $\tilde{W} = \begin{bmatrix} \mathbf{u}_{c_1} & \mathbf{u}_{c_2} & \cdots \end{bmatrix}$ is then used to factorize the projected length through a QR decomposition to get acces to the upper triangular matrix R:

$$C\tilde{W} = QR \tag{2.28}$$

In that case the projections along each direction are sorted columnwise, i.e $C\mathbf{w_i} = QR_i$ and the linear dependent projections have their pivot set to zero. This pivots finally help to choose the d independent columns as nodal coordinates $[x, y, z]$. At this point the configuration that predominates along all equivalent ones is found and it has:

- minimal but non zero projection lengths,
- maximal rank condition for $\mathbf{D}$, and
- linearly independent projections $[C\mathbf{x}\ C\mathbf{y}\ C\mathbf{z}]$

Ones the structure nodal coordinates have been found, the equilibrium matrix can be computed using Eq. (2.33) and decomposed using a Singular Value Decomposition (SVD):

$$\mathbf{A} = \mathbf{U}\Sigma\mathbf{V}^T \tag{2.29}$$

where the matrices U and V have the following null-spaces as

$$U = \begin{bmatrix} \mathbf{u}_1 & \mathbf{u}_2 & \cdots & | \, \mathbf{m}_1 & \cdots & \mathbf{m}_{dn-r_\Sigma} \end{bmatrix} \tag{2.30}$$

and

$$V = [\mathbf{v}_1\ \mathbf{v}_2 \cdots | \, \mathbf{q}_1 \cdots \mathbf{q}_{b-r_\Sigma}] \tag{2.31}$$

where r_Σ is the rank of the diagonal matrix Σ, $m_i \in \mathbb{R}^{d\times n}$ the vectors of infinitesimal mechanisms and $q \in \mathbb{R}^b$ the states of self-stress, each of which solves the homogeneous equation Eq. (2.13). However, if the structure is not in self-stress state there is no access to the null space of $\mathbf{A}$, normally because it has been calculated from approximated coordinates. it is necessary then to modify $\mathbf{A}$ to be rank deficient applying a matrix operation $\mathbb{R}^{nxd} \rightarrow R^b$ that uses $[\mathbf{x}\ \mathbf{y}\ \mathbf{z}]$ to compute and approximation for a new $\mathbf{q}$.

Supposing the equilibrium is not rank deficient after an approximate nodal coordinates are computed. In this case, none of the V columns is a solution for Eq. (2.13). Nevertheless, the column force-density vector $\mathbf{q}_i$ whose sign entries match with the prototype $\mathbf{q}_0$ is selected as possible solution. If any column has this property then it is necessary to select more than column of solution until the signs match the prototype ones (positive $+$ for tension elements and negative $-$ for compression elements). This update in the force density $\mathbf{q}$ that best fits $\mathbf{q}_0$ can be obtained using a least square fit to calculate the vector coefficient $\tilde{\mathbf{q}}$ that minimized the following quantity:

$$\left\| \left[\mathbf{v}_\mathrm{j} \cdots \mathbf{w}_\mathrm{b}\right] \tilde{\mathbf{q}} - \mathbf{q}^0 \right\|^2 \tag{2.32}$$

for a block of columns $\left[\mathbf{v}_j \cdots \mathbf{v}_b\right]$, such that $\mathbf{q} = \left[\mathbf{v}_j \cdots \mathbf{v}_b\right] \tilde{\mathbf{q}}$. the procedure starts taking the two right most columns of $\mathbf{q}$ and the sign property is checked. If the signs does not match with the prototype $\mathbf{q}_0$ another column is selected and the process is repeated until the sign property is fulfilled.

At this point, a new $\mathbf{q}$ is obtained for the approximated coordinates which states

$$\mathbf{A} = \begin{bmatrix} \mathbf{C}^T \operatorname{diag}(\mathbf{C}\mathbf{x}) \\ \mathbf{C}^T \operatorname{diag}(\mathbf{C}\mathbf{y}) \\ \mathbf{C}^T \operatorname{diag}(\mathbf{C}\mathbf{z}) \end{bmatrix} \approx \mathbf{0}. \tag{2.33}$$

and ensures at least one state $s = 1$ of self-stress for the system. The process is repeated again for the new force-densities until the two rank conditions in Eq. (2.16) and Eq. (2.15) are satisfied. In summary, the form-finding procedure consists on iterating Eq. (2.27), Eq. (2.28) and Eq. (2.32) until this rank conditions are satisfied. The potential null spaces in $\mathbf{D}$ and $\mathbf{A}$ are exploited as to impose the existence of at least one solution[2].

Algorithm Flowchart

The flowchart describing the iterative algorithm used for the numerical form-finding of tensegrity structures is presented in Fig. 2.3. A tensegrity can be then obtained for a d-dimensional space just having an intuitive idea of the nodal connectivity's and type of elements(necessary to build the prototype force-density vector $\mathbf{q_0}$).

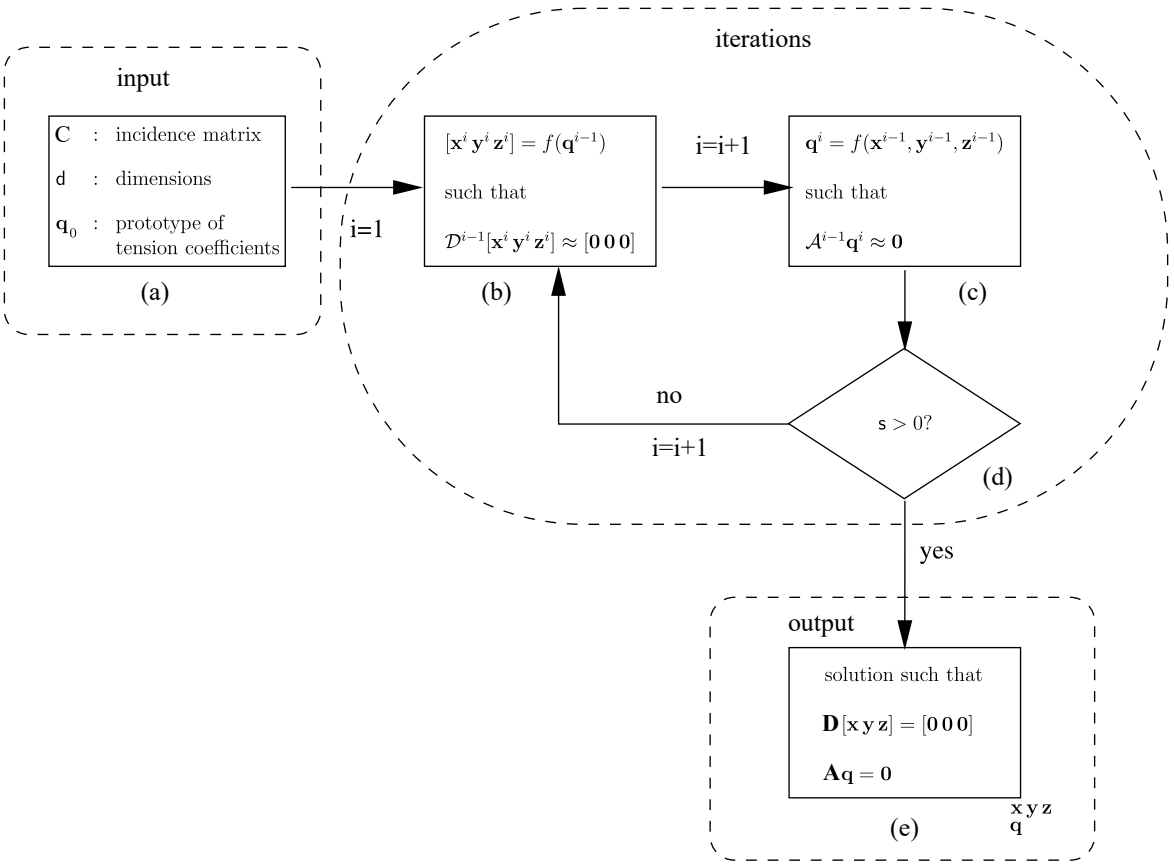

FIGURE 2.3: Flow chart for the numerical form-finding procedure for tensegrity structures[2]

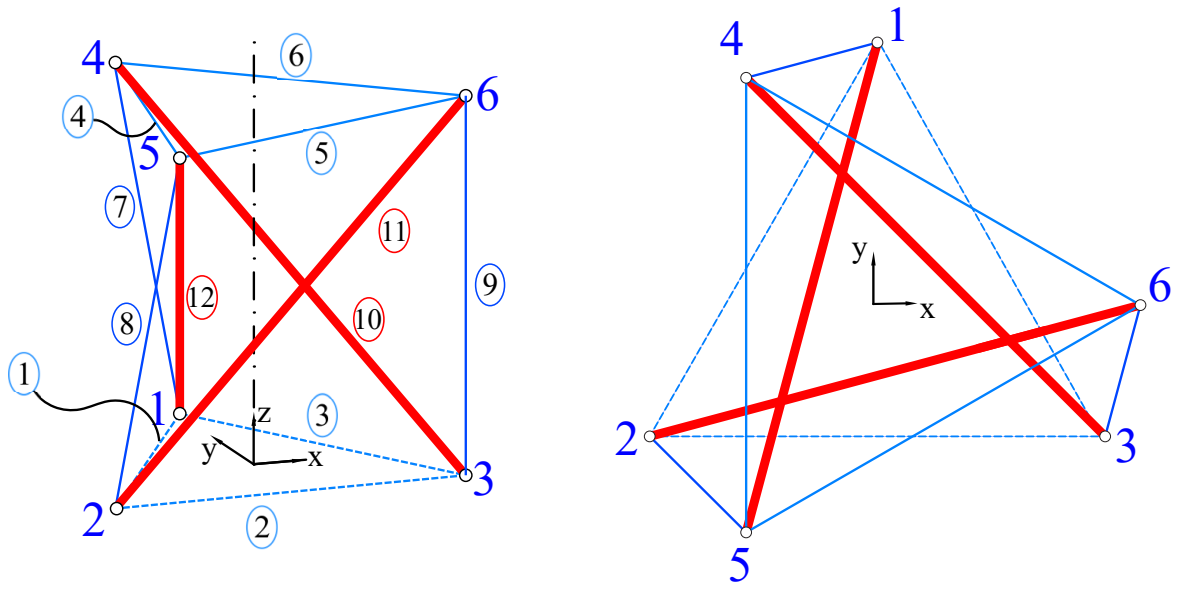

FIGURE 2.4: Nodes and elements forming a 3-strut tensegrity prism

A Matlab code has been implemented where the previous algorithm can be used to build new tensegrity shapes and forms. Due to the interests of this project, the method is used for demonstration purposes on form-finding of tenserities. It is used to determine the shape of 3-strut prism (also known as tensegrity simplex), which is the simplest pure tensegrity structure. Fig. 2.4 shows the way in which the elements are connected for this extensively studied structure:

A tensegrity simplex is composed by 3 bars and 9 cables, interconnected through 6 nodes. The connectivity matrix $\mathbf{C} \in \mathbb{R}^{12\times 6}$ for this structure can be intuitively constructed as:

$$\mathbf{C} = \begin{bmatrix} 1 & -1 & 0 & 0 & 0 & 0 \\ 0 & 1 & -1 & 0 & 0 & 0 \\ 1 & 0 & -1 & 0 & 0 & 0 \\ 0 & 0 & 0 & 1 & -1 & 0 \\ 0 & 0 & 0 & 0 & 1 & -1 \\ 0 & 0 & 0 & 1 & 0 & -1 \\ 1 & 0 & 0 & -1 & 0 & 0 \\ 0 & 1 & 0 & 0 & -1 & 0 \\ 0 & 0 & 1 & 0 & 0 & -1 \\ 1 & 0 & 0 & 0 & -1 & 0 \\ 0 & 1 & 0 & 0 & 0 & -1 \\ 0 & 0 & 1 & -1 & 0 & 0 \end{bmatrix} \tag{2.34}$$

Where for each row representing an element, the two column nodes connected to this element are set to 1 and -1 respectively. Due to the symmetry properties of tensegrities, it is preferivle to set the different groups of structural elements by groups. In this case, the top and bottom cables are the first 6 rows of the matrix, the following 3 rows represent the vertical cables and the last 3 ones are the struts. The initial prototype force density vector $\mathbf{q}_0$ can be constructed then with this consideration as:

$$\mathbf{q}_0 = \begin{bmatrix} 1 & 1 & 1 & 1 & 1 & 1 & 1 & 1 & 1 & -1 & -1 & -1 \end{bmatrix}^T \tag{2.35}$$

The struts or bars are then forced to be in compression while the cables in tension. It will be preferable, due to the mentioned symmetry, that the values for the vertical cables, the force density value takes a different value. Nevertheless, as the objective is to determine the real value of ||, the prototype hypothesis will not be changed. The final input is the problem dimension, which in this case is 3.

At this point, the iterative process starts and the force density matrix **D** can be constructed, and in this case

$$\mathbf{D} = \begin{bmatrix} 2 & -1 & -1 & -1 & 1 & 0 \\ -1 & 2 & -1 & 0 & -1 & 1 \\ -1 & -1 & 2 & 1 & 0 & -1 \\ -1 & 0 & 1 & 2 & -1 & -1 \\ 1 & -1 & 0 & -1 & 2 & -1 \\ 0 & 1 & -1 & -1 & -1 & 2 \end{bmatrix} \tag{2.36}$$

The rank of this matrix is 4, which does not satisfy the rank deficiency condition Eq. (2.16) as $(4 <= 6-3-1)$. This is due to the initial prototype force-density vector. The matrix is then decomposed into its eigenvectors and eigenvalues. Remember that the eigenvector columns are the basis of nodal coordinates to satisfy the equilibrium condition. The potential nullity of the eigenvalues is checked and in this case only two nullity columns are available. Then, the number of columns is incremented at list to $d+1=4$ to have enough candidates to nodal coordinates. This candidates are reduced through the *QR* decomposition to compute the projected length and 2-norm to determine the coordinates for minimum length elements. Finally, from this first part of the iterative process, the set of candidates to nodal coordinates is:

$$[\mathbf{xyz}] = \begin{bmatrix} -0.5543 & -0.0253 & 0.5768 \\ -0.5543 & 0.5122 & -0.2665 \\ -0.5543 & -0.4869 & -0.3103 \\ 0.1614 & 0.2665 & 0.5122 \\ 0.1614 & 0.3103 & -0.4869 \\ 0.1614 & -0.5768 & -0.0253 \end{bmatrix} \tag{2.37}$$

The effectiveness of the reduction method used to determine the candidates to nodal coordinate shows a possible state of self-stress $s=1$ fulfilling the rank condition Eq. (2.16). The Singular Value Decomposition of A gives the tensegrity state of self stress for the given connectivities and coordinates. As only one state of self-stress exists, the last column of possible self stress states is selected, which is:

$$\mathbf{q} = \begin{bmatrix} 0.2041 \\ 0.2041 \\ 0.2041 \\ 0.2041 \\ 0.2041 \\ 0.2041 \\ 0.3536 \\ 0.3536 \\ 0.3536 \\ -0.3536 \\ -0.3536 \\ -0.3536 \end{bmatrix} \tag{2.38}$$

This self-stress vector now leads to a rank deficient force-density matrix **D** and then the tensegrity structure is determined directly in the first iteration. The obtained force density vector, can be normalized for example, dividing by the first element, such that

$$\mathbf{q} = \begin{bmatrix} 1.0000 \\ 1.0000 \\ 1.0000 \\ 1.0000 \\ 1.0000 \\ 1.0000 \\ 1.7321 \\ 1.7321 \\ 1.7321 \\ -1.7321 \\ -1.7321 \\ -1.7321 \end{bmatrix} \tag{2.39}$$

The previous results have been compared with the analytical solution for a simplex tensegrity regarding verification purposes, which is [30]

$$\mathbf{q} = \begin{bmatrix} 1 \\ 1 \\ 1 \\ 1 \\ 1 \\ 1 \\ \sqrt{3} \\ \sqrt{3} \\ \sqrt{3} \\ -\sqrt{3} \\ -\sqrt{3} \\ -\sqrt{3} \end{bmatrix} \tag{2.40}$$

which matches with the normalized values obtained from the numerical form-finding method.

Now this normalized internal force-density coefficients can be multiplied by a pre-stress coefficient p_{s0} (in units of N/m) to set an initial level of pre-stress for the structure. Note that the symmetry behavior of tensegrities is notable. The top and bottom cables are subjected to the same force-density while the vertical cables and struts are subjected to the same but opposite internal force. The latter ensures that the bars are in compression as needed. The visualization of the obtained tensegrity is shown in Fig. 2.5. The obtained structure is exactly the same as shown in Fig. 2.4 and the coordinates can be now placed as desired in space (i.e to have a defined geometry with the 1-2-3 triangle is at the $z = 0$ plane). The found force-density vector is the internal forces that makes the structure self-equilibrated, an then it is mandatory for any structural analysis. As mentioned before, it is possible to normalize it and then scale by a pre-stress factor α to increase the structural rigidity under external loads, as here they are not considered.

To show more demonstrative cases, the developed code was tested for different *know* or already existing tensegrities. First, adding more struts to the same type of prismatic tensegrity and then, overlapping the 3-strut prism to generate a mast.

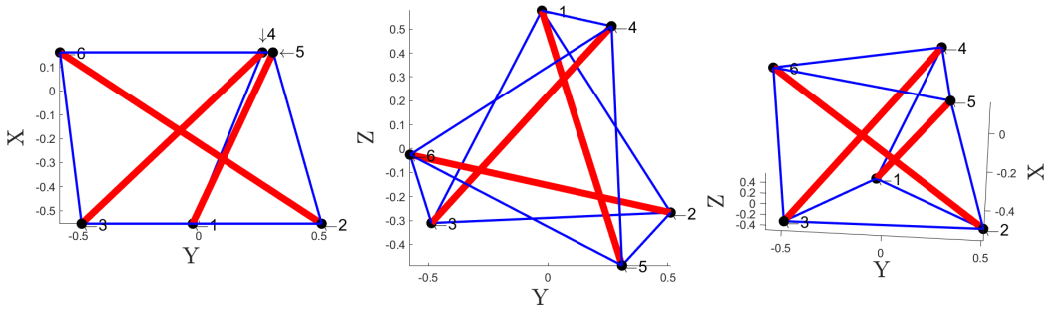

(A) Lateral View (B) Top View (C) Side View

FIGURE 2.5: Different views from the obtained tensegrity structure

The increase the number of struts, it is necessary to intuitively include the new connectivities to generate new C matrix. The connectivity for this type of structures is easy to define using programming software, allowing to simplify the *intuitive* part of this analysis. For a 4-strut tensegrity prism and an 8-strut one, the bottom an top surfaces still have the same area rotate an angle as it can be seen from Fig. 2.6.

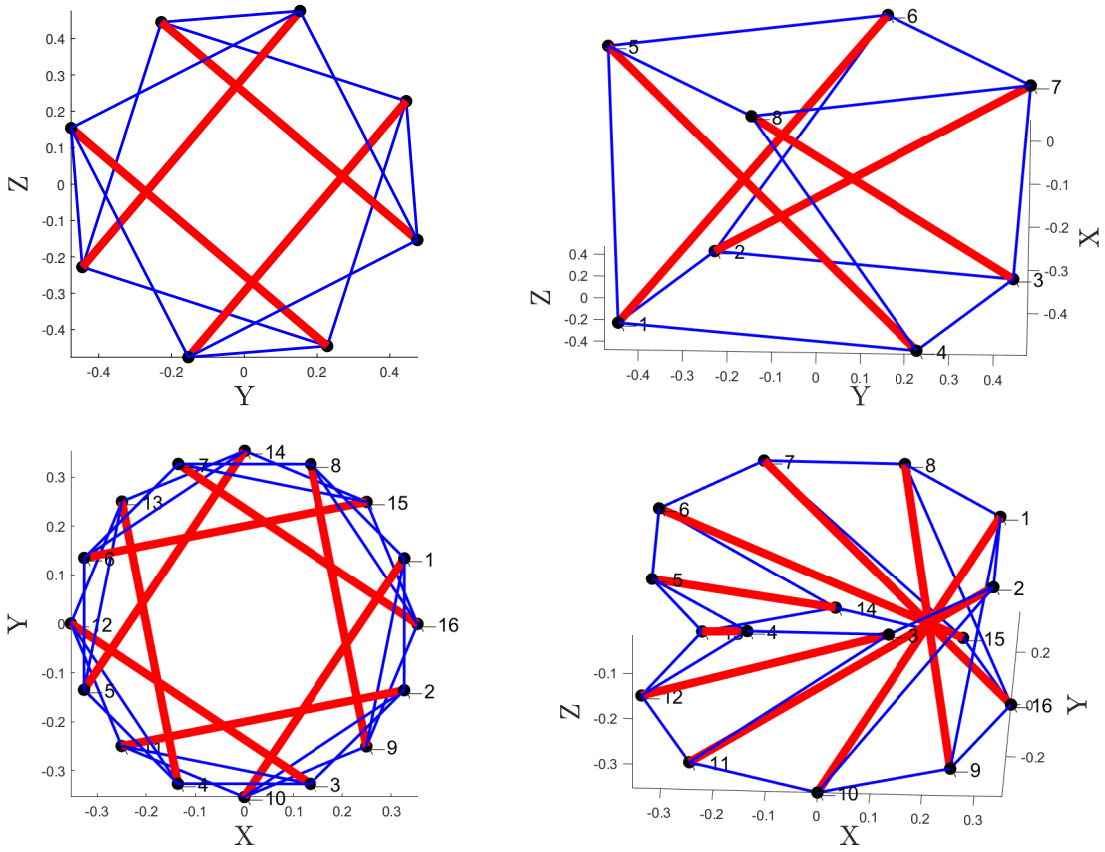

(A) Top View (B) Side View

FIGURE 2.6: Results from the form finding of a 4-strut and 8-strut prism

For the case of 4-strut prism, the force-density vector q states that, in order for the structure to be in equilibrium: bottom and top cables have a normalized force density coefficient of $q_{t,b} = 1$ while lateral cables and struts have a coefficient of $q_{l,s} = 1.4142$ and -1.4142 respectively. The level of internal force-density in the lateral cables (tension) and struts (compression) has been reduced with respect the 3-strut case. For the case of 8-strut prism, top and bottom cables are normalized to $q_{t,b} = 1$ while lateral cables and struts have a force-density coefficient of $q_{l,s} = 0.7654$ and -0.7654 respectively. Again, the traction in lateral cables and compression in struts has been reduced as the number of structural elements is increased (the internal loads are distributed along more elements, reducing the one carried by each of them).

The program has been exploited to determine its ability to develop structures that are coupled to form a mast. To do so, considering the 3-strut prism analyzed before a new connectivity is determined where two of them superimposed to form a two-stage mast. To visualize the impact on the addition of elements during the task of form finding, the following experiment is proposed: initially the simplex structures are directly superimposed using cables (names saddle) to unify both stages and the verical cables of a simplex tensegrity. Then, new cables (namelly diagonal) are introduced in the previous connectivities. Same procedure is finally done by adding a new set of cables into the bottom stage (reinforcing cables).

For the case where only the two simplex are overlapped, the desired form is shown in Fig. 2.7 while the obtained geometry through the form finding process shows the results in Fig. 2.10

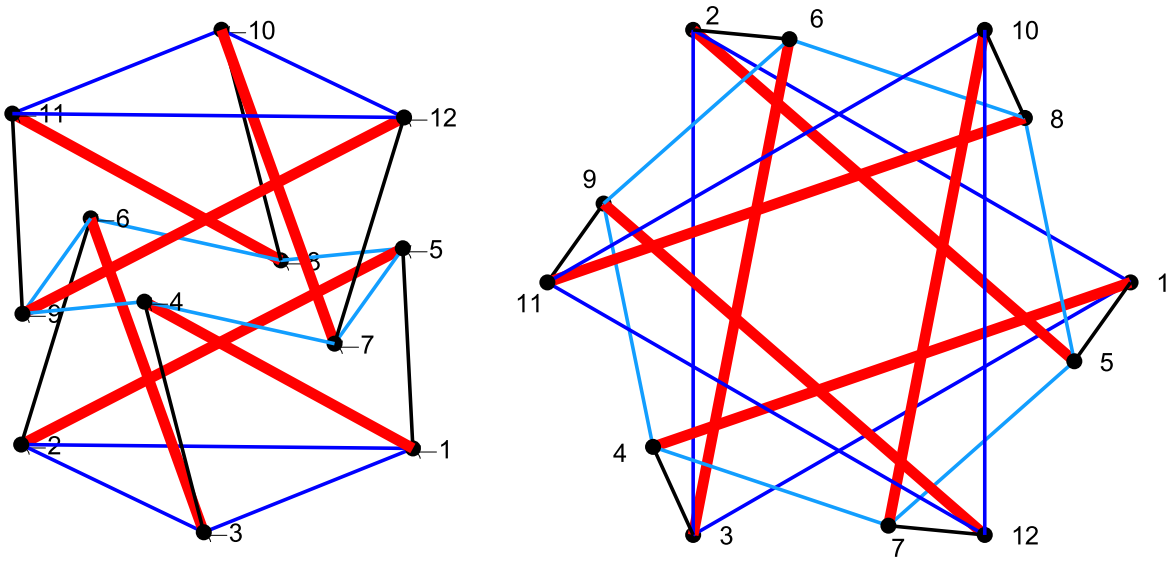

FIGURE 2.7: Shape of the desired two stage mast with only vertical cables

The dark lines represent the top and bottom cables, the cyan ones are the saddle cable, the dark ones represent the vertical cables and the struts are repented by the red lines. The implemented form-finding method leads to a solution for this connectivity topology at the first iteration. Although the structure fulfilling the equilibrium conditions is found, its shape is quasi 2-dimensional, without any interest. However, the bars seems to no intersect or collide between them and then can be considered a tensegrity structure. Fig. 2.8 shows the obtained structure and there are some difficulties to understand it.

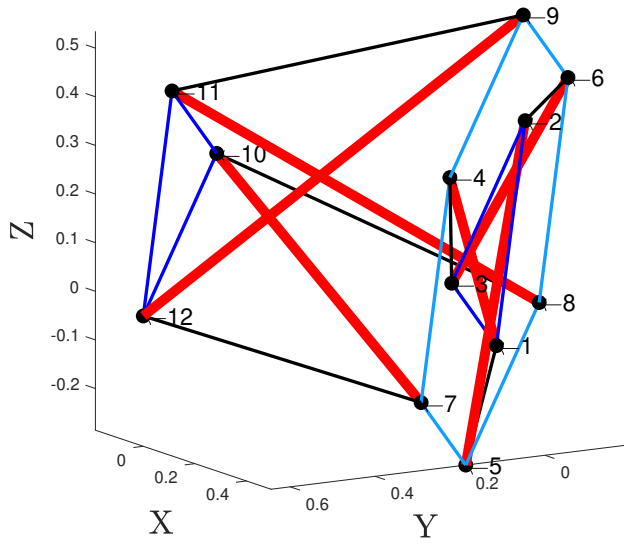

FIGURE 2.8: Results for the shape of a two stage mast with only vertical cables

The same structure is now provided by diagonal cables (green lines in Fig. 2.9) to provide more stiffness to the structure. The results given by the implemented algorithm are shown in Fig. 2.10.

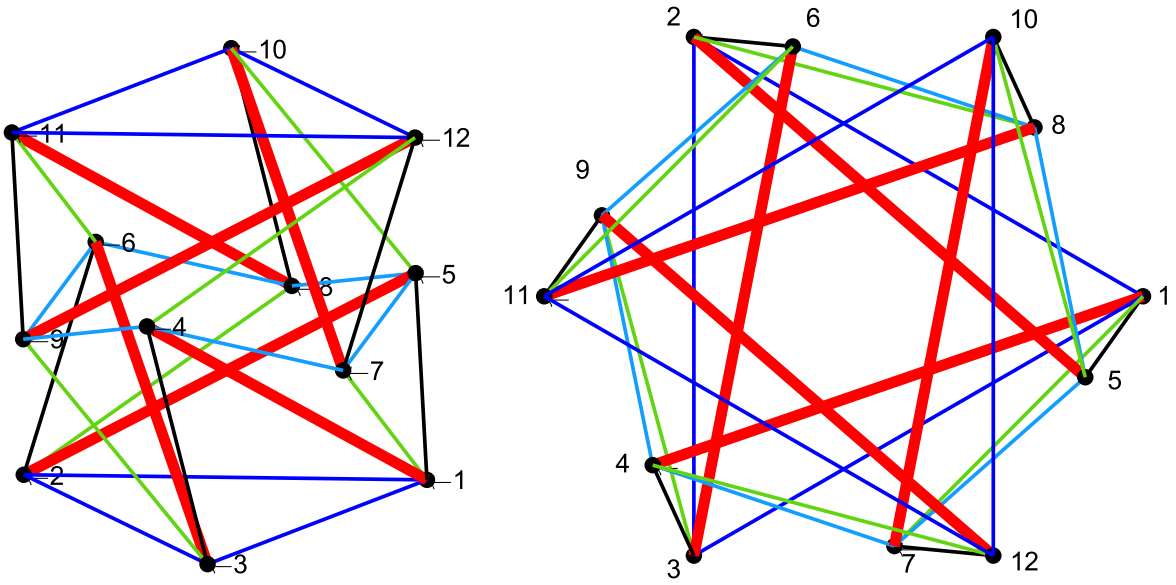

FIGURE 2.9: Desired shape of a tensegrity structure with vertical and diagonal cables

The computed structure this time is entirely 2-dimensional and it cannot be considered a tensegrity structure as the bars and cables are colliding. This fact seems to be corrected when reinforcing cables (dashed lines in Fig. 2.12).

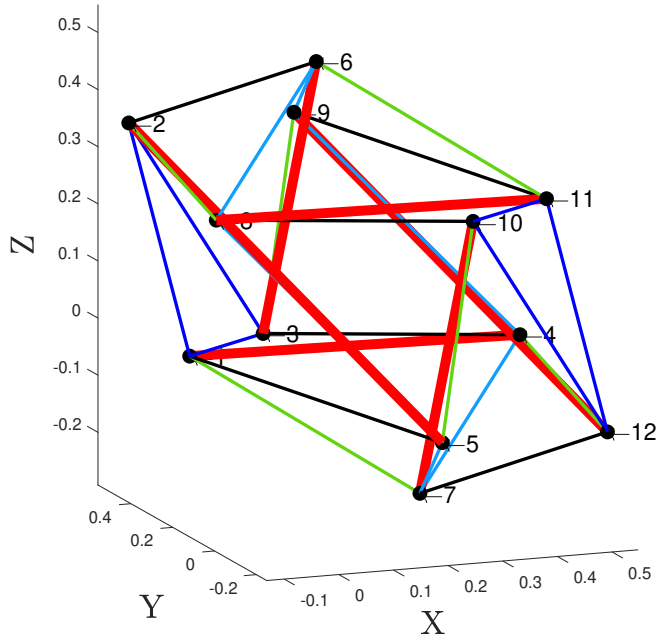

FIGURE 2.10: Results from the form finding of a 2 stage tensegrity mast with vertical cables and diagonal cables

For the case where reinforcing cables are included in the first stage of the structure, the solution becomes 3-dimensional and takes a geometry similar to the one displayed in Fig. 2.11. However, as the algorithm is not constrained to all the possible conditions (location in space, length of elements) the structure found is not symmetric and the self-stress state does not fulfill unilateral behavior. This means that some cables are in tension and compression as well as struts.

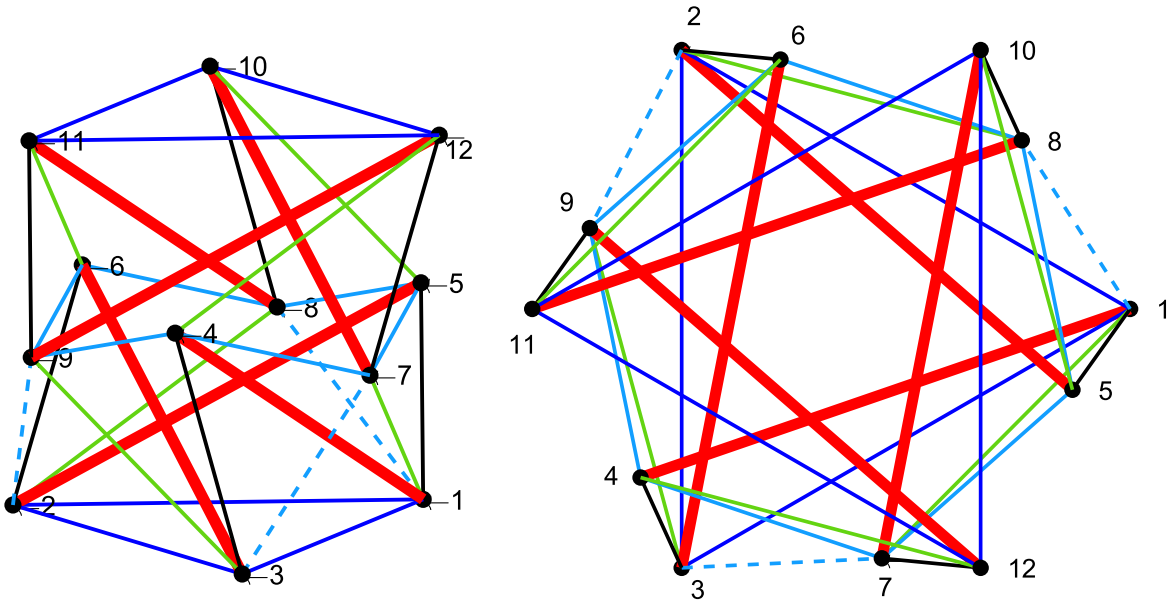

FIGURE 2.11: Desired shape of a tensegrity structure with vertical cables, diagonal cables and reinforcing cables

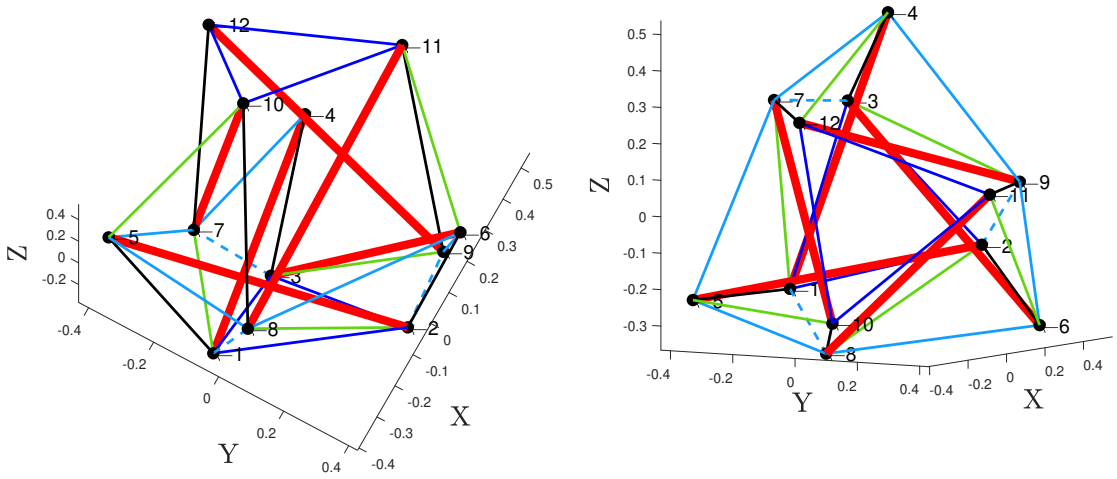

(A) Side View (B) Top View

FIGURE 2.12: Results from the form finding of a 2 stage tensegrity mast with vertical cables, diagonal cables and reinforcing cables

	Normalized force-density q			**Element connectivities for Structure 3**	
Element	**Struct 1**	**Struct 2**	**Struct 3**	**Node 1**	**Node 2**
1	1.0000	1.0000	1.0000	1	2
2	1.0000	1.0000	0.2016	2	3
3	1.0000	1.0000	0.1901	3	1
4	1.0000	1.0000	0.3548	10	11
5	1.0000	1.0000	0.0441	11	12
6	1.0000	1.0000	0.2132	12	10
7	1.0000	1.0000	0.9281	1	5
8	1.0000	1.0000	0.2891	2	6
9	1.0000	1.0000	0.3558	3	4
10	1.0000	1.0000	-0.0050	7	12
11	1.0000	1.0000	0.0980	8	10
12	1.0000	1.0000	0.2621	9	11
13	1.0000	1.0000	0.7878	4	7
14	1.0000	1.0000	0.5663	5	8
15	1.0000	1.0000	-0.2290	6	9
16	1.0000	1.0000	0.4372	4	9
17	1.0000	1.0000	0.4241	5	7
18	1.0000	1.0000	-0.0629	6	8

19	1.0000	1.0000	0.4386	1	7
20	1.0000	1.0000	0.6973	2	8
21	1.0000	1.0000	-0.3715	3	9
22	-1.0000	1.0000	0.3123	4	12
23	-1.0000	1.0000	0.5288	5	10
24	-1.0000	1.0000	0.0869	6	11
25	-1.0000	-1.5000	-0.8771	1	8
26	-1.0000	-1.5000	0.9818	2	9
27	-1.0000	-1.5000	-0.4960	3	7
28		-1.5000	-0.7563	1	4
29		-1.5000	-0.9472	2	5
30		-1.5000	-0.0158	3	6
31			-0.4389	7	10
32			-0.3181	8	11
33			-0.1963	9	12

TABLE 2.2: Normalized pre-stress coefficient for different structures.

Although this method is a fast way where a simple algorithm is needed to determine the form-finding of a tensegrity structure, it suffers from different drawbacks [1], which are:

- As the vectors of tension coefficients and coordinates are selected from the null-space o the equilibrium matrices **A** and **D**, we do not have control over the length units.
- By defining the tensegrity configuration by using a incidence matrix **C** and ensuring that the initial tension coefficient vector **q** (i.e a prototype vector where the cables have a coefficient of 1 and bars a coefficient of -1), the procedure finds a tensegrity structure in the first iterations (first iteration for 3D Class 1 structures), otherwise the model fails by not leading to a valid structure for the defined dimension (i.e a 3D structure collapses into a 2D one). Also, for non-uniform tension vectors the iterations required by the program to find a tensegrity are increased.
- For complex tensegrities, the aesthetics of the structure is notably reduced and then symmetry properties are lost.

Regarding this drawbacks it is necessary to define other methods which allow us to build tensegrities with a desired shape and structural value. This is way normally analytical and semi-analytical models are used for this purpose. In this project, the reduced coordinates method is also studied to generate a tensegrity mast composed by two 3-strut simplex tensegrities overlapped. For this method, the initial location of the nodes is introduced in symbolic form and for a given design parameters, the solution is found for the overlap. This method is extensively explained in Section 2.4.

2.3 Initial Self-Stress Design

In most of the existing method for form-finding of tensegrity structures, the previous methodology and similar ones have been used to determine novel shapes in view of aesthetic and mechanical properties. The determination of the stress distribution to

appropriately stabilize the structure for a given shape is called initial self-stress design [31].

Normally a tensegrity structure can have more than one states of self-stress ($s > 1$). Due to this, the member forces can be expressed as linear combination of this self-stress states. Sometimes, the vectorial bases obtained from the null space of the equilibrium matrix does not take into account unilateral behavior. As a consequence, it is necessary to determine a suitable state of self-stress for a given topology. When the initial state of self-stress is determined, the structure can be analyzed (statically, dynamically).

For a known structure shape (nodal coordinates) and connectivities, the equilibrium matrix A can be constructed and decomposed using Singular Value Decomposition. The number of states of self-stress is given by the rank of this matrix.

$$\mathbf{A} = \mathbf{U}\Sigma\mathbf{V}^T \tag{2.41}$$

As already seen, the last s columns of matrix $\mathbf{V}$ represent the right null-space vector of the equilibrium matrix $\mathbf{A}$. According to the number of self-stress states, two situations are given.

CASE I - $(s = 1)$

If the number of states of self-stress is equal to 1, then no extra calculations have to be made as only one right null-space vector solution (satisfying self-equilibrium equations) is given. This is the situation for the studied structures in the numerical form-finding. The force-density $\mathbf{q}$ obtained from this solution may force the cables to carry tensions while the bars carry compression. Since this force-density vector values are relative, it can be multiplied by -1 to carry unilateral behavior.

CASE II - $(s > 1)$

If there is more than one number of states of self-stress ($s > 1$), there are s number of independent states of self-stress, and they do not necessarily satisfy the unilateral behavior of elements. In such case, the force density vector has to be determined as a linear combination of the last s columns of matrix $\mathbf{V}$.

$$\mathbf{q} = c_1\mathbf{v}_{m-s+1} + c_2\mathbf{v}_{m-s+2} + c_3\mathbf{v}_{m-s+3} + \cdots + c_s\mathbf{v}_m \tag{2.42}$$

where c is the vector coefficients for s independent self-stress modes. For convenience and simplicity, the matrix $\mathbf{G}$ is defined as:

$$\mathbf{c} = \begin{Bmatrix} c_1 & c_2 & \cdots & c_s \end{Bmatrix} \tag{2.43}$$

$$\mathbf{V} = \begin{bmatrix} \mathbf{v}_1 & \mathbf{v}_2 & \cdots & \mathbf{v}_{r_A} & | \, \mathbf{v}_{m-n_s+1} & \mathbf{v}_{m-n_s+2} & \cdots \mathbf{v}_m \end{bmatrix} \tag{2.44}$$

$$\mathbf{G} = \begin{bmatrix} \mathbf{g}_1 & \mathbf{g}_2 & \cdots & \mathbf{g}_s \end{bmatrix} = \begin{bmatrix} \mathbf{v}_{m-s+1} & \mathbf{v}_{m-s+2} & \cdots & \mathbf{v}_m \end{bmatrix} \tag{2.45}$$

the force density vector $\mathbf{q}$ can be now written as

$$\mathbf{q} = \mathbf{G}\mathbf{c} \tag{2.46}$$

As the matrix $\mathbf{G}$ does not carry the elements information type, it does not take into account the unilateral behavior between elements. This problem can be solved if we consider symmetry groups of elements which carry the same amount of force-density. This geometric symmetry can be found by identifying the members in similar positions, same length and carrying integral force-density. Then, h symmetry groups can be created and the force-density vector can be expressed as:

$$\mathbf{q} = \left\{ \begin{array}{cccccccc} q_1 & q_1 & \cdots & q_i & q_i & \cdots & q_h & q_h \end{array} \right\}^T = \left[\begin{array}{ccccc} 1 & 0 & 0 & 0 & 0 \\ \vdots & 1 & 0 & 0 & 0 \\ 0 & \vdots & 1 & 0 & 0 \\ 0 & 0 & \vdots & 1 & \vdots \\ 0 & 0 & 0 & \vdots & 1 \end{array} \right] \left[\begin{array}{c} q_1 \\ \vdots \\ q_i \\ \vdots \\ q_h \end{array} \right] \tag{2.47}$$

and more compactly as

$$\mathbf{q} = \left\{ \begin{array}{ccccc} q_1 & \cdots & q_i & \cdots & q_h \end{array} \right\}^T = \left[\begin{array}{ccccc} \mathbf{e}_1 & \cdots & \mathbf{e}_i & \cdots & \mathbf{e}_h \end{array} \right] \left[\begin{array}{c} q_1 \\ \vdots \\ q_i \\ \vdots \\ q_h \end{array} \right] \tag{2.48}$$

where $\mathbf{q}_i$ represents the force-density value for the group of symmetry i, and $\mathbf{e}_i$ represents a column vector which entries are 1 for the ith group of symmetry while the others are zero. Introducing Eq. (2.48) into Eq. (2.46) yields

$$c_1\mathbf{g}_1 + c_2\mathbf{g}_2 + \cdots + c_{n_s}\mathbf{g}_{n_s} - \mathbf{e}_1 q_1 - \mathbf{e}_2 q_2 - \cdots - \mathbf{e}_h q_h = \mathbf{0} \tag{2.49}$$

and in matrix form

$$\overline{\mathbf{G}}\overline{\mathbf{c}} = \mathbf{0} \tag{2.50}$$

where

$$\overline{\mathbf{G}} = \left[\begin{array}{ccccccccc} \mathbf{g}_1 & \mathbf{g}_2 & \cdots & \mathbf{g}_{n_s} & -\mathbf{e}_1 & \cdots & -\mathbf{e}_i & \cdots & -\mathbf{e}_h \end{array} \right] \tag{2.51}$$

and

$$\overline{\mathbf{c}} = \left\{ \begin{array}{cccccccc} c_1 & c_2 & \cdots & c_{n_s} & q_1 & \cdots & q_i & \cdots & q_h \end{array} \right\}^T \tag{2.52}$$

The solution for this system lies in the null-space of matrix $\overline{\mathbf{G}}$. This solution is normally a vector column with the c_i coefficients and the force-densities for each group of symmetry. The last step is to set the adequate values for each element depending on its group of symmetry. This ensures unilateral behavior along the entire structure.

The initial self-stress design or force-finding method has been used in static analysis of tensegrity structures. It allows us to determine an initial state of self-stress for a given

structure without the influence of external loads.

In the following section, another method for form-finding is presented. This method is used to determine the self-equilibrium condition for a given tensegrity structure topology. It different from analytical form-finding because the structure is already known and the length of the bars and cables can be controlled for design purposes.

2.4 Reduced Coordinates Method

The numerical form-finding studied in the previous section has some disadvantages due to constraint which are not considered. This problem can be solved by the reduced coordinates methods for form-finding, introduced by sultan *et al.* [28]. Imagine that we have a tensegrity structure with b elements (M cables and O struts). The struts are supposed to be a set of bilateral constraints acting on a structure of cables. Then, a set of N independent generalized coordinates $g = (g_1\ g_2\ ...\ g_N)^T$ is introduced to define the position and orientation of the struts.

For the said structure, consider a state of self-stress and let t_j denote the axial force in a generic cable element j. The force in the cables $t = (g_1\ g_2\ ...\ g_M)^T$ are in equilibrium with the adequate forces in the struts and no external loads. From virtual work, a set of equilibrium equations relating the forces in the cables, but without showing explicitly the forces acting inside the struts can be obtained.

Consider a virtual displacement $\delta\mathbf{g}$ on the structure which does not involve extension of the struts. The length of the cable j will change so that

$$\delta l_j = \sum_{i=1}^{N} \frac{\partial l_j}{\partial g_i} \delta g_i \tag{2.53}$$

and considering all cables

$$\delta\mathbf{l} = \mathbf{A}^{\mathrm{T}} \delta\mathbf{g} \tag{2.54}$$

where the element of the $N \times M$ equilibrium matrix A are:

$$A_{ij} = \frac{\partial l_j}{\partial g_i} \tag{2.55}$$

As the struts are considered rigid inelastic bodies, their extension is zero and the virtual work in the struts is also zero. The total internal work then comes by hand of the cables, which is defined as

$$\mathbf{t}^{\mathrm{T}} \delta\mathbf{l} = (\mathbf{A}\mathbf{t})^{\mathrm{T}} \delta\mathbf{g} \tag{2.56}$$

As already mentioned, the equilibrium condition is achieved when the previous expression is zero for any virtual displacement δg, and then:

$$\mathbf{A}\mathbf{t} = \mathbf{0} \tag{2.57}$$

where t is the normalized internal force vector. The previous equation has no trivial solution if and only if

$$\operatorname{rank} \mathbf{A} < M \tag{2.58}$$

Where only entirely positive solutions are of interest, i.e

$$t_j > 0 \text{ for } j = 1, 2, \ldots, M \tag{2.59}$$

Chapter 3

Static Analysis of Truss Structures

3.1 Linear Finite Element Method

In this section the classical FEM for truss structures is presented by implementing the Direct Stiffness Method. The equations in matrix form for a pin-jointed structure can be obtained from the individual equilibrium study of the different members. Fig. 3.1 shows an isolated truss element e, of length l_e subjected only to axial forces F_1^e and F_2^e.

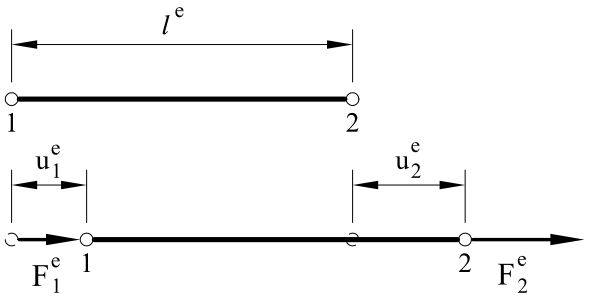

FIGURE 3.1: Truss element with 2 nodes in a 2D space

Same notation as in the *3-D* algorithm bars for Computational Engineering notes is used here. The strain at any point along the element is defined by the strength of the material, i.e

$$\varepsilon = \frac{\Delta l^e}{l^e} = \frac{u_2^e - u_1^e}{l^e} \tag{3.1}$$

where u_1^e and u_2^e are the nodal displacements at nodes 1 and 2. The strain along the element is related to the strain through the Hooke's law [REF] as:

$$\sigma = E^e \varepsilon = E^e \frac{u_2^e - u_1^e}{l^e} \tag{3.2}$$

where E^e is the material Young Modulus. If we cut transversely the bar element e, the axial force N at that section can be obtained by integrating the stress over the cross sectional area. This axial force in a structure is transmitted along to the adjacent bars through the joints. If the material is homogeneous then:

$$N = A^{(e)} \sigma = (EA)^{(e)} \frac{u_2^{(e)} - u_1^{(e)}}{l^{(e)}} \tag{3.3}$$

The equilibrium nodal equations for the bar in Fig. 3.1 is simply:

$$F_1^e + F_2^e = 0 \tag{3.4}$$

with

$$F_2^e = N = (EA)^e \frac{u_2^e - u_1^e}{l^e} = \kappa^e (u_2 - u_1) \tag{3.5}$$

where $\kappa = E^e A^e / l^e$ and the previous equilibrium equations for the element written in matrix form become:

$$\mathbf{F}^e = \left\{ \begin{array}{c} F_1^e \\ F_2^e \end{array} \right\} = k^e \left[\begin{array}{cc} 1 & -1 \\ -1 & 1 \end{array} \right] \left\{ \begin{array}{c} u_1^e \\ u_2^e \end{array} \right\} = \mathbf{K}^e \mathbf{u}^e \tag{3.6}$$

where $\mathbf{K}^e$ is the bar stiffness matrix, which depends on the geometry of the bar (l^e, A^e) and its mechanical properties (E^e). $\mathbf{u}^e = [u_1, u_2]^T$ and $\mathbf{F}^e = [F_1, F_2]^T$ are the small displacements and the joint equilibrium force vector for the bar element, respectively.

It is possible to write the equilibrium equations for an entire structure by imposing the equilibrium of forces at each of the n joints, i.e

$$\sum_{e=1}^{n_e} F_i^e = F_j \quad , \quad j = 1, n \tag{3.7}$$

The summation on the left hand side of (3.7) extends over all the n_e bars sharing the joint point with the global number j and F_j^{ext} is the external load acting on that joint. The values of the bar end forces R_i^e can be expressed in terms of the joint displacement, leading to the following global equilibrium equation:

$$\left[\begin{array}{cccc} K_{11} & K_{12} & \cdots\cdots & K_{1n} \\ K_{21} & K_{22} & \cdots\cdots & K_{2n} \\ \vdots & & & \\ \vdots & & & \\ K_{n1} & K_{n2} & \cdots\cdots & K_{nn} \end{array} \right] \left\{ \begin{array}{c} u_1 \\ u_2 \\ \vdots \\ \vdots \\ u_n \end{array} \right\} = \left\{ \begin{array}{c} f_1 \\ f_2 \\ \vdots \\ \vdots \\ f_n \end{array} \right\} \tag{3.8}$$

which in vector-matrix form is:

$$\mathbf{K}\mathbf{u} = \mathbf{f} \tag{3.9}$$

where $\mathbf{K}$ is known as the global stiffness matrix, u and f the nodal global displacements and global force vectors respectively. The computation of the global stiffness matrix is known as assembly process.

The stiffness matrix derived in Eq. (3.6) corresponds to a 1D linear elastic truss. This stiffness matrix can be derived for a 2D or 3D truss element using the a transformation matrix. For a 3D element with 3 degrees of freedom per node:

$$\mathbf{R}^e = \frac{1}{l^e} \left[\begin{array}{cccccc} x_2^e - x_1^e & y_2^e - y_1^e & z_2^e - z_1^e & 0 & 0 & 0 \\ 0 & 0 & 0 & x_2^e - x_1^e & y_2^e - y_1^e & z_2^e - z_1^e \end{array} \right] \tag{3.10}$$

and the stiffness matrix in global coordinates for this case becomes then from

$$\mathbf{K}^e = \mathbf{R}^{e\top}\mathbf{K}^{e'}\mathbf{R}^e \tag{3.11}$$

where

$$\mathbf{K}^{e'} = \frac{A^e E^e}{l^e}\begin{bmatrix} 1 & -1 \\ -1 & 1 \end{bmatrix} \tag{3.12}$$

and the element length is found through the coordinates x, y and z of nodes 1 and 2.

$$l^e = \sqrt{\left(x_2^e - x_1^e\right)^2 + \left(y_2^e - y_1^e\right)^2 + \left(z_2^e - z_1^e\right)^2} \tag{3.13}$$

For this method, it is possible to include the pre-stress by modeling it as an internal force. In local coordinates, the internal force vector is:

$$F_{int}{}^{e'} = f_i\begin{bmatrix} 1 \\ -1 \end{bmatrix} \tag{3.14}$$

where f_{int} is the internal tension in each element. This can be expressed in terms of global coordinates using the same transformation matrix $\mathbf{R}^e$.

$$\mathbf{F}_{int}^e = \mathbf{R}^{e\top}\mathbf{F}_{int}^{e'} \tag{3.15}$$

The objetive of this project is not to explain the entire FEM method and some parts will be assumed to be know. The next step now is to assemble the global stiffness matrix, the global internal force vector and global external force vector if there is. The solution for the dispalcements is determined by a mandatory set of boundary conditions. Some degrees of freedom are fixed (they will not suffer displacements) and then, the reduced stiffness and reduced force vector for the non-fixed DOFs are used to determine the structure displacements.

3.2 Extension to Non-Linear FEM

Classically, spatial reticulated system are studied with the hypothesis of small deformations and displacements which leads to a linearization of their behavior under external loads. Then the study explained in the previous section is considered sufficient. However, depending upon mechanical properties the elements, levels of external loads or just structural specifications, other hypothesis have to be taken into account for: (i) the material behavior and (ii) the magnitude of the displacements [12]. The study then remain into the geometrical and non-linear analysis of the structure.

When talking about tensegrity structures, they are considered as spatial reticulated systems. Due to the presence of pre-stress between the elements to stabilize the structure, they exhibit geometric non-linearity.

The development of a nonlinear has the same basis the model for a truss structure but now including the geometric non-linearity of the system. The assumptions for this model are:

- The elements composing the structure can only carry axial loads.
- Cables can only carry tension while struts or bars carry compression loads. This ensures a unilateral element behavior.

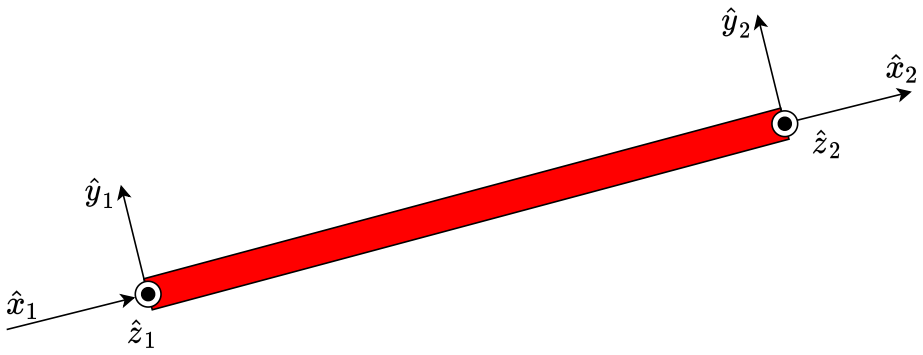

FIGURE 3.2: Truss element with two nodes in a 3-D space

- The loads are applied at the nodes.
- From the form-finding part, the nodal coordinates of the structure and the normalized force-density vector are known. This allows us to determine initial pre-stress of the structure under no loads but with a self equilibrated structure.

Imagine the 3-dimensional space truss shown in Fig. **??**, with two nodes at each end and the local axes are $\hat{x}$, $\hat{y}$ and $\hat{z}$. The strain energy of the element is written as

$$U_e = \frac{1}{2}\int_0^{l_e} \sigma_{\hat{x}}\varepsilon_{\hat{x}} A d\hat{x} \tag{3.16}$$

where l_e and A are the length and cross-sectional area of the element respectively, σ is the axial stress and ε the axial strain. The relation between the strain and stress has been seen in Eq. (3.2). The strain energy becomes then:

$$U_e = \frac{1}{2}\int_0^{L} EA\varepsilon_{\hat{x}}^2 d\hat{x} \tag{3.17}$$

where E is the Young Modulus or elasticity modulus of the element. To account for large deformations and displacements quadratic terms must be introduced. The exial strain is then written as

$$\varepsilon = \frac{\partial \hat{u}}{\partial \hat{x}} + \frac{1}{2}\left[\left(\frac{\partial \hat{u}}{\partial \hat{x}}\right)^2 + \left(\frac{\partial \hat{v}}{\partial \hat{x}}\right)^2 + \left(\frac{\partial \hat{w}}{\partial \hat{x}}\right)^2\right] \tag{3.18}$$

where $\hat{u_i}$, $\hat{u_j}$ and $\hat{u_k}$ represent the nodal displacement in $\hat{x}$, $\hat{y}$ and $\hat{z}$ directions respectively. Along the truss element the nodal displacement have a linear variation and then the derivation in Eq. (3.18) can be written as:

$$\frac{\partial \hat{u}}{\partial \hat{x}} = \frac{\Delta \hat{u}}{\Delta \hat{x}} = \frac{\hat{x}_2 - \hat{x}_1}{L}$$
$$\frac{\partial \hat{v}}{\partial \hat{x}} = \frac{\Delta \hat{v}}{\Delta \hat{x}} = \frac{\hat{y}_2 - \hat{y}_1}{L}$$
$$\frac{\partial \hat{w}}{\partial \hat{x}} = \frac{\Delta \hat{w}}{\Delta \hat{x}} = \frac{\hat{z}_2 - \hat{z}_1}{L}$$

Substituting back into Eq. (3.18) and ignoring the cubic and higher order terms:

$$U_e = \frac{1}{2}EAL\left[\left(\frac{\hat{x}_2-\hat{x}_1}{L}\right)^2 + \frac{\partial\hat{u}}{\partial\hat{x}}\left\{\left(\frac{\hat{x}_2-\hat{x}_1}{L}\right)^2 + \left(\frac{\hat{y}_2-\hat{y}_1}{L}\right)^2 + \left(\frac{\hat{z}_2-\hat{z}_1}{L}\right)^2\right\}\right] \tag{3.19}$$

At this point, the partial derivative $\partial\hat{u}/\partial\hat{x}$ can be approximated as:

$$\frac{\partial\hat{u}}{\partial\hat{x}} \approx \varepsilon_{\hat{x}} = \frac{\sigma_{\hat{x}}}{E} = \frac{T}{EA} \tag{3.20}$$

where T is the element pre-stress force. The value of T will depend on the element type (positive for cables in tension and negative for bars in compression). Rearranging terms, the strain energy of the two node struss element becomes

$$U_e = \frac{1}{2}\frac{EA}{L}(\hat{x}_2-\hat{x}_1)^2 + \frac{1}{2}\frac{T}{L}\left\{(\hat{x}_2-\hat{x}_1)^2 + (\hat{y}_2-\hat{y}_1)^2 + (\hat{z}_2-\hat{z}_1)^2\right\} \tag{3.21}$$

If a vector of nodal coordinates containing a row with the coordiantes of each node is introduced as $\overline{\mathbf{u}} = \{\hat{x}_1,\hat{y}_1,\hat{z}_1,\hat{x}_2,\hat{y}_2,\hat{z}_2\}^T$, the quadratic terms in Eq. (3.21) can be expressed as:

$$(\hat{x}_2-\hat{x}_1)^2 = (\hat{x}_2-\hat{x}_1)^T(\hat{x}_2-\hat{x}_1) = \overline{\mathbf{u}}^T\begin{Bmatrix}-1\\0\\0\\1\\0\\0\end{Bmatrix}\begin{Bmatrix}-1 & 0 & 0 & 1 & 0 & 0\end{Bmatrix}\overline{\mathbf{u}} \tag{3.22}$$

$$(\hat{x}_2-\hat{x}_1)^2 = \begin{bmatrix}1 & 0 & 0 & -1 & 0 & 0\\ 0 & 0 & 0 & 0 & 0 & 0\\ 0 & 0 & 0 & 0 & 0 & 0\\ -1 & 0 & 0 & 1 & 0 & 0\\ 0 & 0 & 0 & 0 & 0 & 0\\ 0 & 0 & 0 & 0 & 0 & 0\end{bmatrix} \tag{3.23}$$

The same procedure is repeated for the other two quadratic terms in $\hat{y}$ and $\hat{z}$ directions. Doing so and substituting in Eq. (3.21), the strain energy is finally expressed as:

$$U_e = \frac{1}{2}\overline{\mathbf{u}}^T\overline{\mathbf{K}}_L\overline{\mathbf{u}} + \frac{1}{2}\overline{\mathbf{u}}^T\overline{\mathbf{K}}_{NL}\overline{\mathbf{u}} \tag{3.24}$$

where $\overline{\mathbf{K}}_L$ and $\overline{\mathbf{K}}_{NL}$ are the linear and non linear stiffness matrices respectively [38, 41, 42]. Both components represent the tangent stiffness matrix of the element. The linear component represents the material stiffness matrix, normally used for small-deformation truss, and the nonlinear component is the geometrical stiffness matrix caused by pre-stresses, (Guest, 2006). They are expressed as:

$$\overline{\mathbf{K}}_L = \frac{EA}{L}\begin{bmatrix} 1 & 0 & 0 & -1 & 0 & 0 \\ 0 & 0 & 0 & 0 & 0 & 0 \\ 0 & 0 & 0 & 0 & 0 & 0 \\ -1 & 0 & 0 & 1 & 0 & 0 \\ 0 & 0 & 0 & 0 & 0 & 0 \\ 0 & 0 & 0 & 0 & 0 & 0 \end{bmatrix}$$
$$\overline{\mathbf{K}}_{NL} = \frac{T}{L}\begin{bmatrix} 1 & 0 & 0 & -1 & 0 & 0 \\ 0 & 1 & 0 & 0 & -1 & 0 \\ 0 & 0 & 1 & 0 & 0 & -1 \\ -1 & 0 & 0 & 1 & 0 & 0 \\ 0 & -1 & 0 & 0 & 1 & 0 \\ 0 & 0 & -1 & 0 & 0 & 1 \end{bmatrix} \tag{3.25}$$

This new geometric matrix shows the effect of pre-stress in the element and it is *isotropic* at each node [53, 54]. The stiffness matrix in local coordinates for the truss element is:

$$\overline{\mathbf{K}} = \overline{\mathbf{K}}_L + \overline{\mathbf{K}}_{NL} \tag{3.26}$$

For an assembly of elements, the stiffness matrix of the structure is determined by expressing the local coordinates $\overline{\mathbf{X}}$ in terms of global coordinates $\mathbf{X}$. To do so, explained for the linear FEM procedure, transformation matrices are needed. The relation between local and global coordinates is given by

$$\overline{\mathbf{X}} = \mathbf{T}\mathbf{X} \tag{3.27}$$

where the transformation matrix $\mathbf{T}$ is given by

$$\mathbf{T} = 1/L\begin{bmatrix} l_1 & m_1 & n_1 & 0 & 0 & 0 \\ l_2 & m_2 & n_2 & 0 & 0 & 0 \\ l_3 & m_3 & n_3 & 0 & 0 & 0 \\ 0 & 0 & 0 & l_1 & m_1 & n_1 \\ 0 & 0 & 0 & l_2 & m_2 & n_2 \\ 0 & 0 & 0 & l_3 & m_3 & n_3 \end{bmatrix} \tag{3.28}$$

and the direction cosines for the transformation matrix considering a truss element are

$$\begin{aligned} l_1 &= \frac{x_2 - x_1}{L} \\ m_1 &= \frac{y_2 - y_1}{L} \\ n_1 &= \frac{z_2 - z_1}{L} \end{aligned} \tag{3.29}$$

where the other direction cosines are not taken into account since do not appear in the final stiffness matrix expression. The other four rows can be then set to zero. This procedure can be also repeated for the external loads in local coordinates so that

$$\overline{\mathbf{F}}_{ext} = \mathbf{T}\mathbf{F}_{ext} \tag{3.30}$$

where $\overline{\mathbf{F}}_{ext}$ and $\mathbf{F}_{ext}$ are the external loads force vector in local and global coordinates repectively. For a typical structural system, the relation between the external loads and the displacements is given by the relation in Eq. (3.9) as

$$\overline{\mathbf{F}}_{ext} = \overline{\mathbf{K}}\overline{\mathbf{u}} \tag{3.31}$$

and implementing the transformation matrix as in Eq. (3.30)

$$\mathrm{TF_{ext}} = \overline{\mathbf{K}}\mathrm{Tu} \tag{3.32}$$

and re-arrenging

$$\mathbf{F_{ext}} = \mathbf{T}^{-1}\overline{\mathbf{K}}\mathbf{Tu} \tag{3.33}$$

As the transformation matrix is orthogonal, they obey te property $\mathbf{T}^{-1} = \mathbf{T}^{T}$. Therefor,

$$\mathbf{F_{ext}} = \mathbf{T}^{T}\overline{\mathbf{K}}\mathbf{Tu} \tag{3.34}$$

As a result, the stiffness matrix in global coordinates can be expressed as:

$$\mathbf{K} = \mathbf{T}^{T}\overline{\mathbf{K}}\mathbf{T} \tag{3.35}$$

The linear and geometric stiffness matrices for each individual element need to be expressed in coordinates associated with global axes. After this transformation, this two matrices are summed as in Eq. (3.36) to represent the overall stiffness of the system. The traditional FEM assembly process is used to asseble the global stiffness matrix as

$$\mathbf{K} = \mathbf{K}_{L} + \mathbf{K}_{NL} \tag{3.36}$$

It is important to note that the geometric matrix is invariant to transformation and then then $\overline{\mathbf{K}}_{NL}$ is already expressed in global coordinates.

The final consideration to close the nonlinear FEM method is the consideration of the internal forces acting on a pre-stressed system. For the truss element in figure 3.2, the internal force vector with respect to local coordinates is:

$$\overline{\mathbf{F}}_{int} = T\left\{\begin{array}{cccccc} -1 & 0 & 0 & 1 & 0 & 0 \end{array}\right\} \tag{3.37}$$

and in global coordinates with the same transformation matrix $\mathbf{T}$

$$\mathbf{F}_{int} = \mathbf{T}^{T}\overline{\mathbf{F}}_{int} \tag{3.38}$$

Following the same line as for the global stiffness matrix, the internal force vector can be assembled for an entire structure. The solution for the displacements is given by imposing some boundary conditions as already mentioned and solving for the reduced matrices.

3.3 Static Analysis with External Loads

As mentioned before, the study of the behavior of a tensegrity structure under external loads has a nonlinear solution and then an iterative method is required. If the structure is under external loads, large deformations and/or deformation in it can occur, and then the structure stiffness level will be changed. If the loads are huge enough, the cables of a tensegrity structure may go slack and the structure stiffness will be reduced, or the distribution of forces in the structure may considerably change, affecting stiffness [34].

A Newthon Raphson algorithm is considered as best option for this nonlinear analysis. The process starts setting an external load and iterating for this load until a solution that stabilizes the system is obtained. For each iteration, the stiffness matrix is recomputed for te deformed struture. The non-linear relationship between displacements and external forces is then:

$$\mathbf{K}_T\mathbf{u} = \mathbf{F}_{ext} - \mathbf{F}_{int} \tag{3.39}$$

The condition of equilibrium is achieved when internal forces equal the external ones. This is then the convergence condition for the resolution of the system.

From the form-finding process, the normalized force-density vector $\mathbf{q}$ for the structure to be in self-equilibrium has been obtained. With this, the initial internal force for element i in a pre-stressed structure is obtained as:

$$p_{s0}q_iL_i = T_i = \frac{E_iA_i}{L_{0,i}}(L_i - L_{0,i}) \tag{3.40}$$

where p_{s0} is the coefficient of pre-stress force, denoting the level of initial pre-stress of the structure(units of force per unit length). The rest length of the element $L_{0,i}$ of the element can be then computed for a given pre-stress level p_{s0} as

$$L_{0,i} = \frac{E_iA_iL_i}{E_iA_i + T_i} = \frac{E_iA_iL_i}{E_iA_i + p_{s0}q_iL_i} \tag{3.41}$$

At this point, all the required data to build the stiffness matrices and internal force vector per element in global coordinates is determined. The assembly of the global $\mathbf{K}$ and $\mathbf{F}_{int}$ can be now done considering two nodes per element and 3 degrees of freedom (DOF) per node.

The problem now can be solved just considering the internal forces and the initial displacements can be obtained. This initial displacements will be caused by the internal forces and the initial pre-stress level p_{s0} considered. The problem then starts when an external load is introduced to the system. Note that this external load is considered to be assembled as well as the internal force vector (the loads are directly set into the corresponding DOF direction). For this load, the solution for Eq. (3.39) is obtained and the displacements are computed. The new nodal coordinates due to this displacements are determined as:

$$\mathbf{X} = \mathbf{X}_0 + u \tag{3.42}$$

where $\mathbf{X}_0$ denotes the initial (or previous) coordinates of the structure and u the displacement due to influence of an external load (sol for Eq. (3.39)). Again, the length of each element is computed and the internal forces-densities (force per unit length) updated using Hookes Law [4] as in Eq. (3.40)

$$q_i = \frac{E_iA_i}{L_{0,i}L_i}(L_i - L_{0,i}) \tag{3.43}$$

and the new element pre-stress force T is obtained multiplying by the new length of elements (force units). Finally, the global stiffness matrix is then assembled such as the global internal force vector. The force balance for each node is done by computing the norm of $\mathbf{F}_{ext} - \mathbf{F}_{int}$. The process for the same external load is repeated until the norm is under a pre-defined tolerance. Then, the external force is increased and the process is repeated

again. When a number of iterations N is achieved denoting the final range of increasing external load, the process is finished.

Flow Chart Diagram

A program using Matlab has been developed following the algorithm described and shown in the following flow chart.

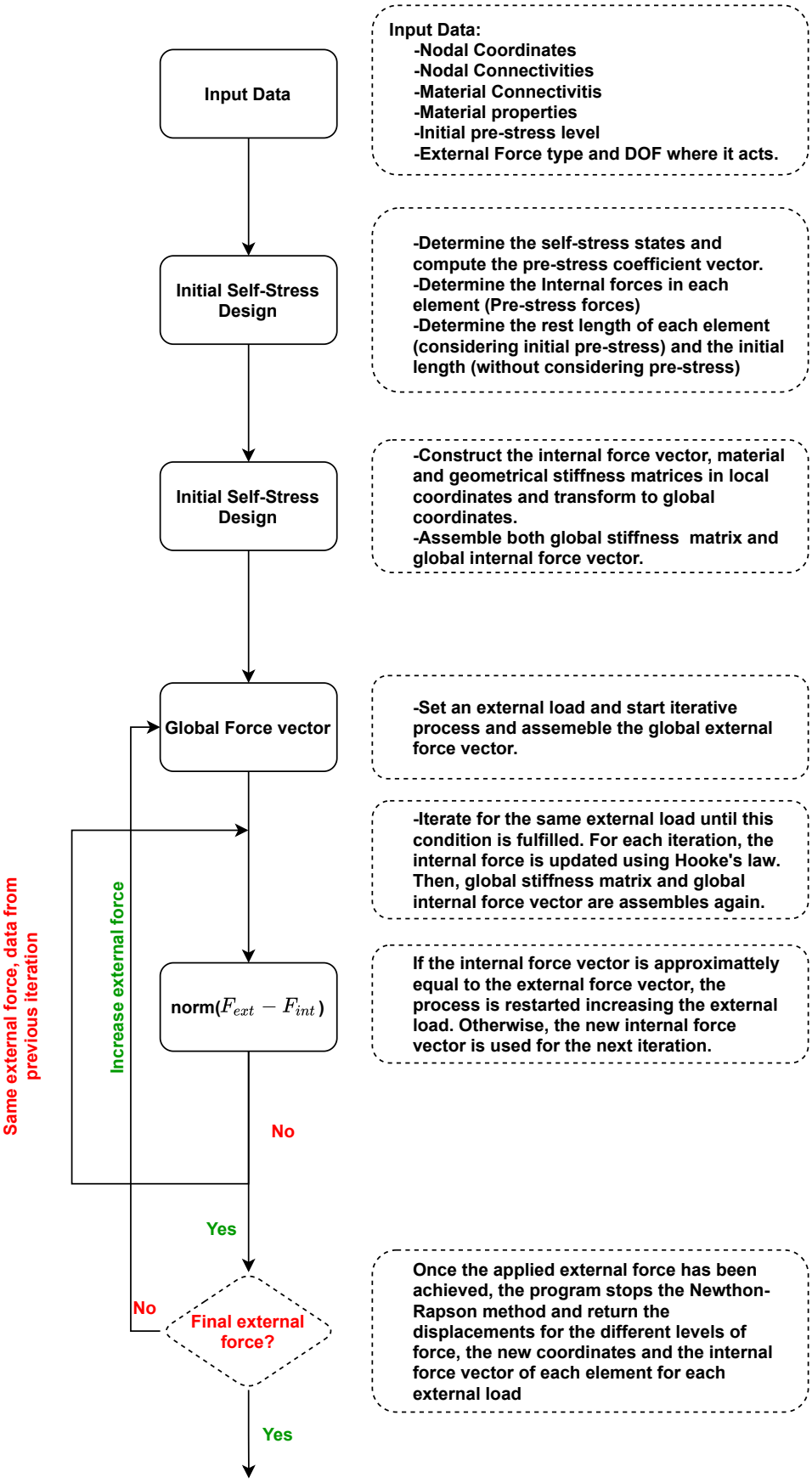

FIGURE 3.3: Flowchart Diagram for the non-linear FEM method

3.3.1 Program Test

The validation of the program has been done following the research of Kebiche *et all* [12] where a simple tensegrity cell, composed by four struts and 12 cables. Several external loads have been applied to the tensegrity in order to determine its behavior against traction and compression, flexion and torsion loads. The following figure shows the tensegrity connectivities and the defined scenario:

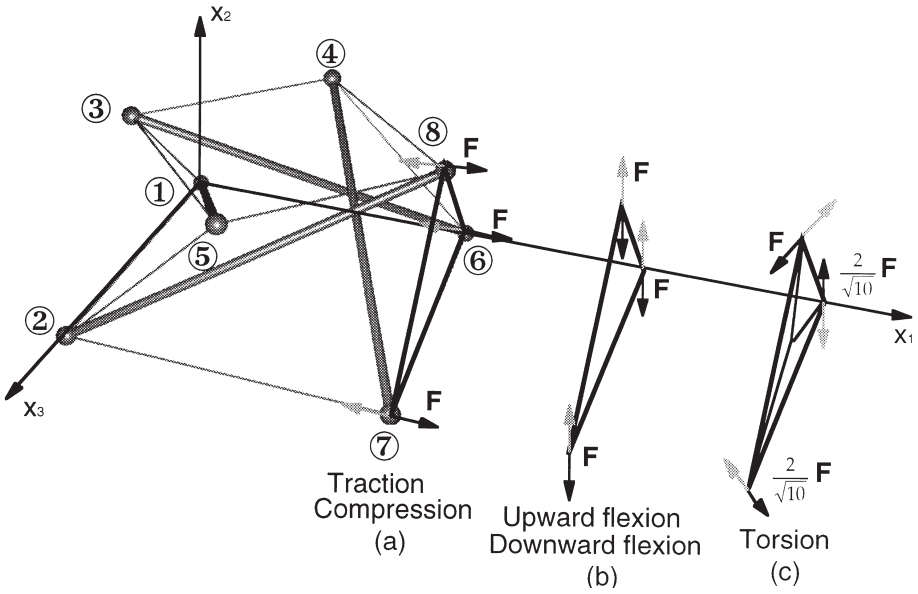

FIGURE 3.4: Geometry of the four-strut tensegrity system and different load cases [12]

The considered structure has the following nodal coordinates in *cm* units.

Node	x	y	z	**Node**	x	y	z
1	0	100	0	**5**	50	0	50
2	0	0	0	**6**	100	100	0
3	0	50	50	**7**	100	0	0
4	50	100	50	**8**	100	50	50

TABLE 3.1: Nodal Coordintes of the tensegrity structure in Fig. 3.4

Following the Force-Finding method explained in Chapter **??**, the connectivity matrix **C** of the structure is determined and the equilibrium equation A is built. The SVD decomposition of A states the number of self stress states for this structure is $s = 1$. This is then used to determine the force-density matrix and again the SVD decomposition of it done in order to determine force-density for each group of symmetry (which in this case are four: 4 bottom cables, 4 top cables, 4 diagonal cables and 4 struts). The initial pre-stress level selected for this problem is $p_{s0} = 55\ N/cm$. The rest length (without pre-stress) is then computed and compared with the real initial one (without no pre-stress). the data at this point of the problem is summarized in the following table:

Element	Nodes		Nature	Self-stress Coeff. q_0	Length L^e[cm]	Rest L. L_0^e[cm]	Internal stress T [N]
1	1	6		1	100	99.51	5500
2	2	7	Lower	1	100	99.51	5500
3	1	2	cables	1	100	99.51	5500
4	6	7		1	100	99.51	5500
5	3	4		2	70.71	70.22	7778.17
6	3	5	Upper	2	70.71	70.22	7778.17
7	4	8	cables	2	70.71	70.22	7778.17
8	5	8		2	70.71	70.22	7778.17
9	2	5		2	70.71	70.22	7778.17
10	7	8	Bracing	2	70.71	70.22	7778.17
11	4	6	cables	2	70.71	70.22	7778.17
12	1	3		2	70.71	70.22	7778.17
13	3	6		-2	122.47	122.72	−13472.18
14	2	8	Struts	-2	122.47	122.72	−13472.18
15	1	5		-2	122.47	122.72	−13472.18
16	4	7		-2	122.47	122.72	−13472.18

TABLE 3.2: Elements, nodal connectivities and initial properties.

For the present tensegrity, the geometrical and mechanical characteristics are:

Element Type	Young Modulus E [GPa]	Cross-section A [cm^2]
Cables	40	0.28
Struts	200	0.325

TABLE 3.3: Element properties

The boundary conditions for this problems states that: the node number 1 is totally fixed, the node number 2 can only move along y direction (x_2 in Fig. 3.4) and the node number 3 can move in y, z directions. This means that our boundary conditions restrict: the first three DOFs of node 1, the first and third DOFs of node 2 and the first DOF of node number 2.

$$\mathbf{FIX}_{DOF} = [1 \;\; 2 \;\; 3 \;\; 4 \;\; 6 \;\; 7] \tag{3.44}$$

The external loads are considered to act over nodes number 6, 7 and 8. The non-linear stiffness procedure has been implemented for the different types of load.

1. Results for Traction and Compression

For this case, the external loads are applied in the x direction (positive for traction and negative for compression). The interval for the external load varies from $F = \pm 2\ kN$. Kebiche increments the external load by a factor of 3 ($3F$) for each iteration, so then the range becomes $F = \pm 6\ kN$. Fig. 3.5 shows the evolution of the mean displacements on nodes number 6, 7 and 8 for different ranges of external loads along x axis.

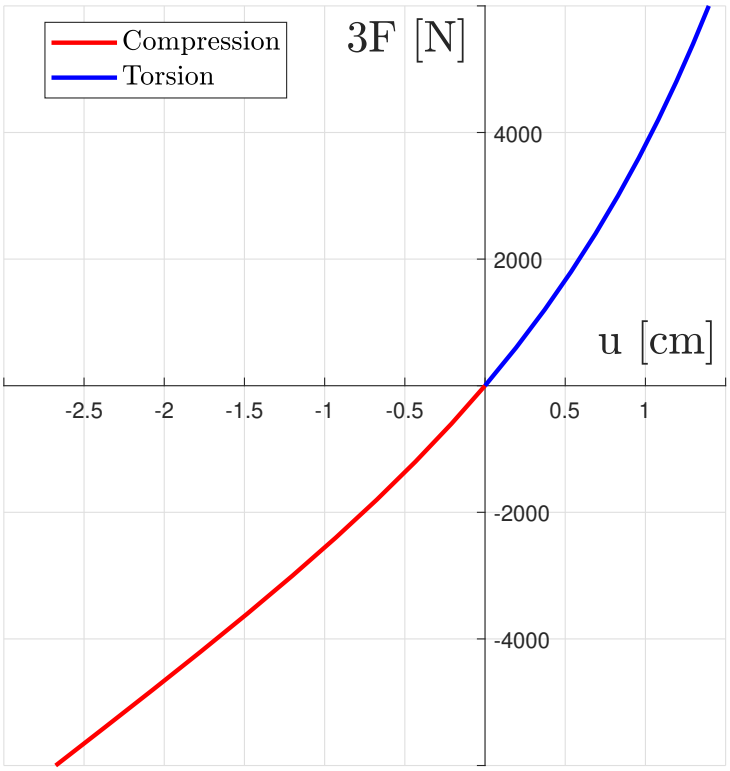

FIGURE 3.5: Behavior of the structure under compression and traction loads. Average displacements of nodes 6,7,8 in the load application direction

As it can be seen, the behavior described by the structure is non-linear, and those linearities are not the same according to whether this structure is subjected to traction or compression. In traction, the system becomes stiffer as the external load increases, i.e, the displacements are smaller. This stiffness is progressively lost if the structure is compressed, showing an *anisotropic behaviour* [12] for this four-strut tensegrity.

To better visualize the displacements, the deformed four-strut tensegrity structure when maximal load is plotted over its initial configuration (dashed gray lines) in Fig. 3.9. The response of the structure to traction loads is stiffer than the case of compression loads, as explained before. The structure then if the load is increased will be deformed faster if compression is applied.

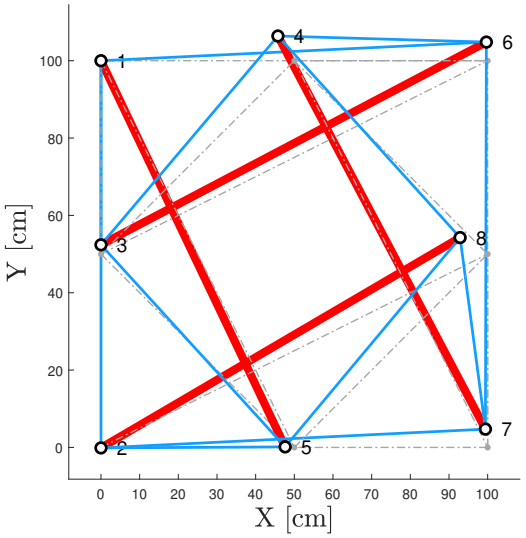

(A) Traction Load - Top view

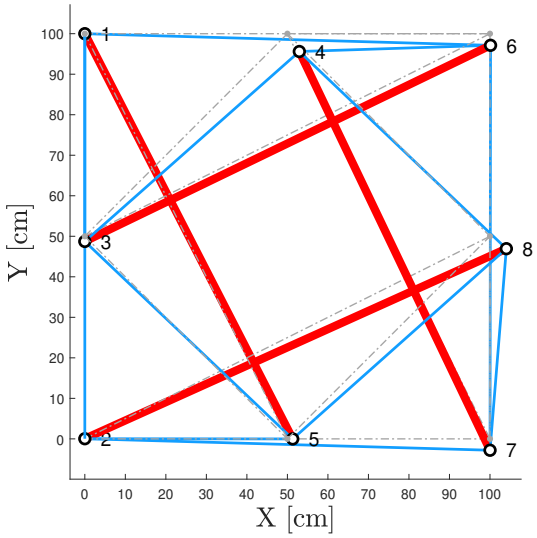

(B) Compression Load - Top view

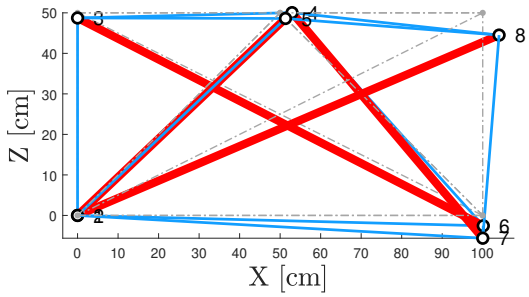

(C) Traction Load

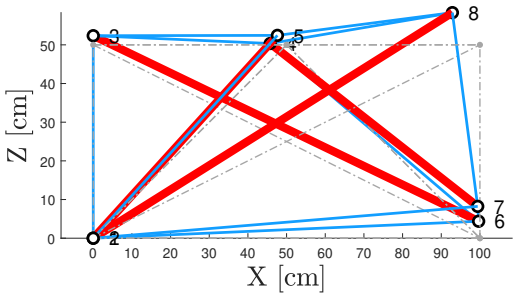

(D) Compression Load

FIGURE 3.6: Top and lateral views of the deformed structure under compression and traction loads.

The evolution of the internal stress (in N/m^2) each element is also presented in Fig. **??**. The difference between this evolution for cables and struts is notorious depending on the type of load, compression or traction. For a given traction external load, a big increase in the stress(and then internal tension) in cables number 1 and 2 is noticed as they are oriented in the same direction of load application. Simultaneously, a decrease in elements 3 and 4 occurs as they are orthogonal to the load. Regarding the compression loads, the internal stress in the bars increases significantly. This fact can be the result of buckling in struts, which is less important for traction loads.

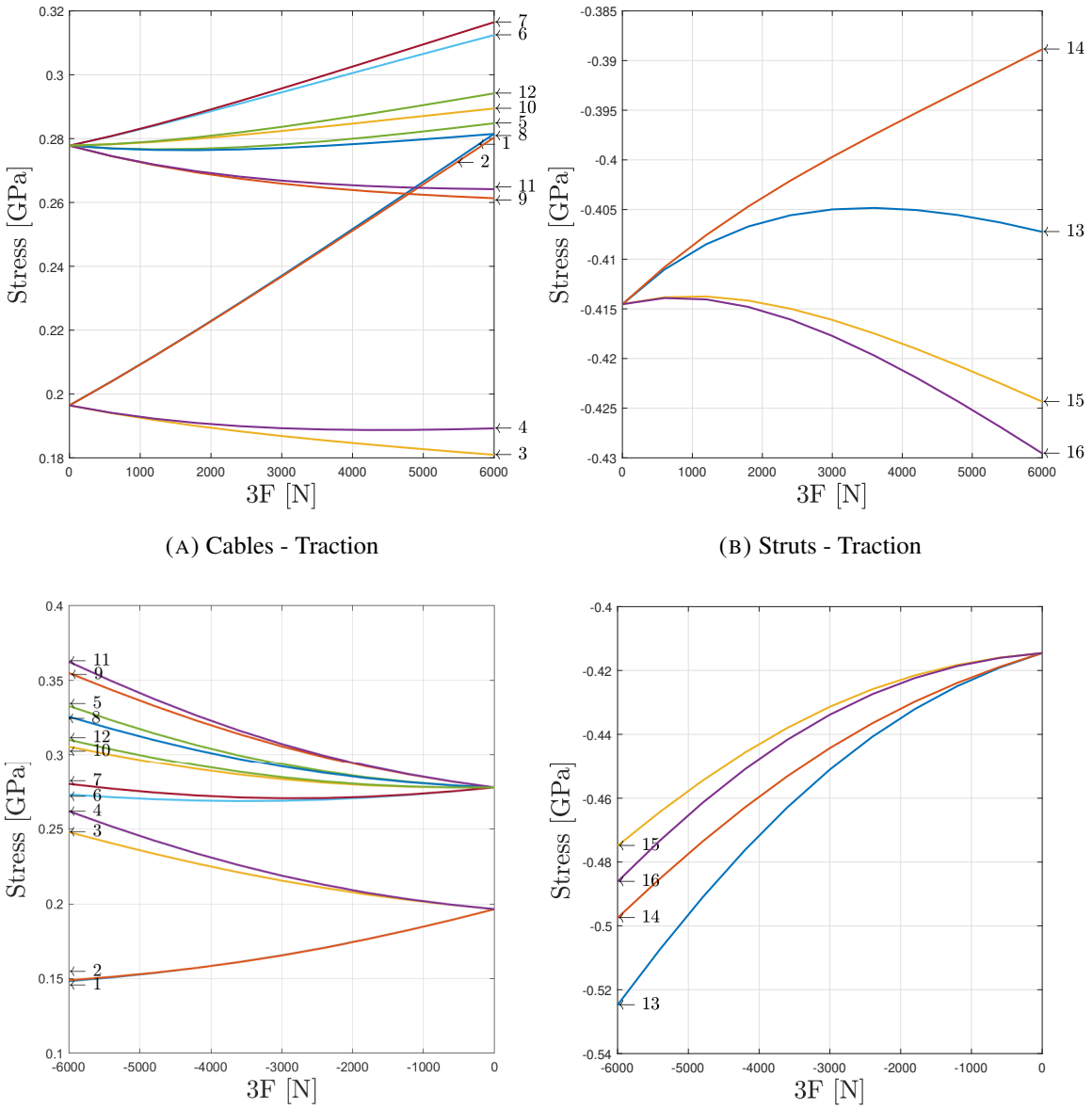

(A) Cables - Traction

(B) Struts - Traction

(C) Cables - Compression

(D) Struts - Compression

FIGURE 3.7: Evolution of the internal stress in members under Traction and Compression loads.

2. Results for Flecxion Up and Down

The same procedure has been followed as for compression-traction loads, but now considering flexion loads. As it can be seen in Fig. 3.4, this loads are applied in the positive z-direction(Upward flexion) and negative z-direction(Downward flexion). The behavior of the structure under flexion using the same range of 0 to 6 kN is shown in figure Fig. 3.8

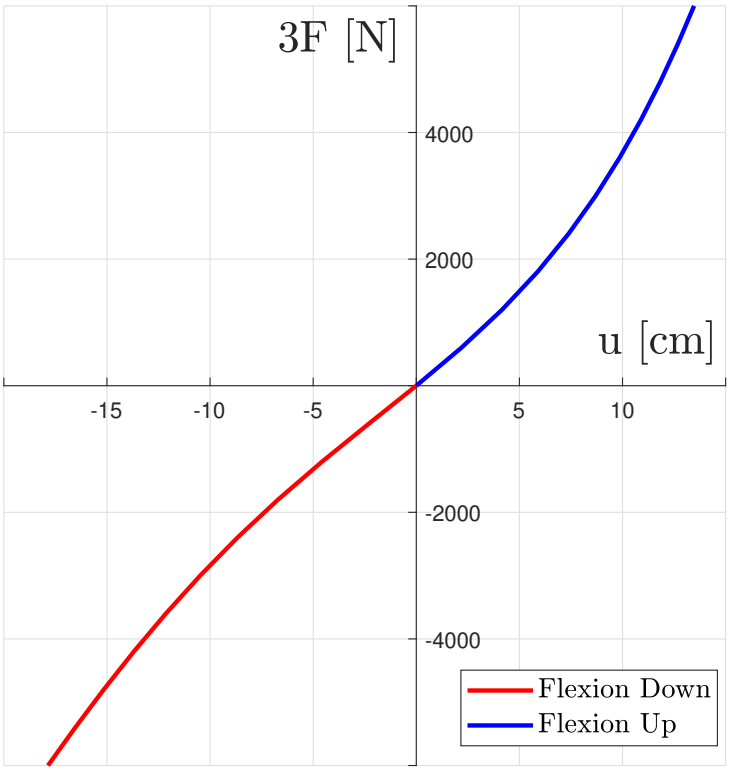

FIGURE 3.8: Behavior of the structure under flexion loads. Average displacements of nodes 6,7,8 in the load application direction

Again the nonlinear behavior is present, showing a stiffer structure as long as external loads increase. This fact is present in the upward flexion direction and in less ratio for the downward direction, showing also *anisotropic* behavior as in the case of compression-traction loads. This can be due to the difference in the initial internal force vector shown in Tab. (3.2), which is two times higher for the upper cables than the lower ones. For a load value of 6 kN, the displacements for upward flexion load are 12.8 cm and up 17.26 cm for the downward case. Then, the four-strut tensegrity system stiffness is of low order for torsional loads.

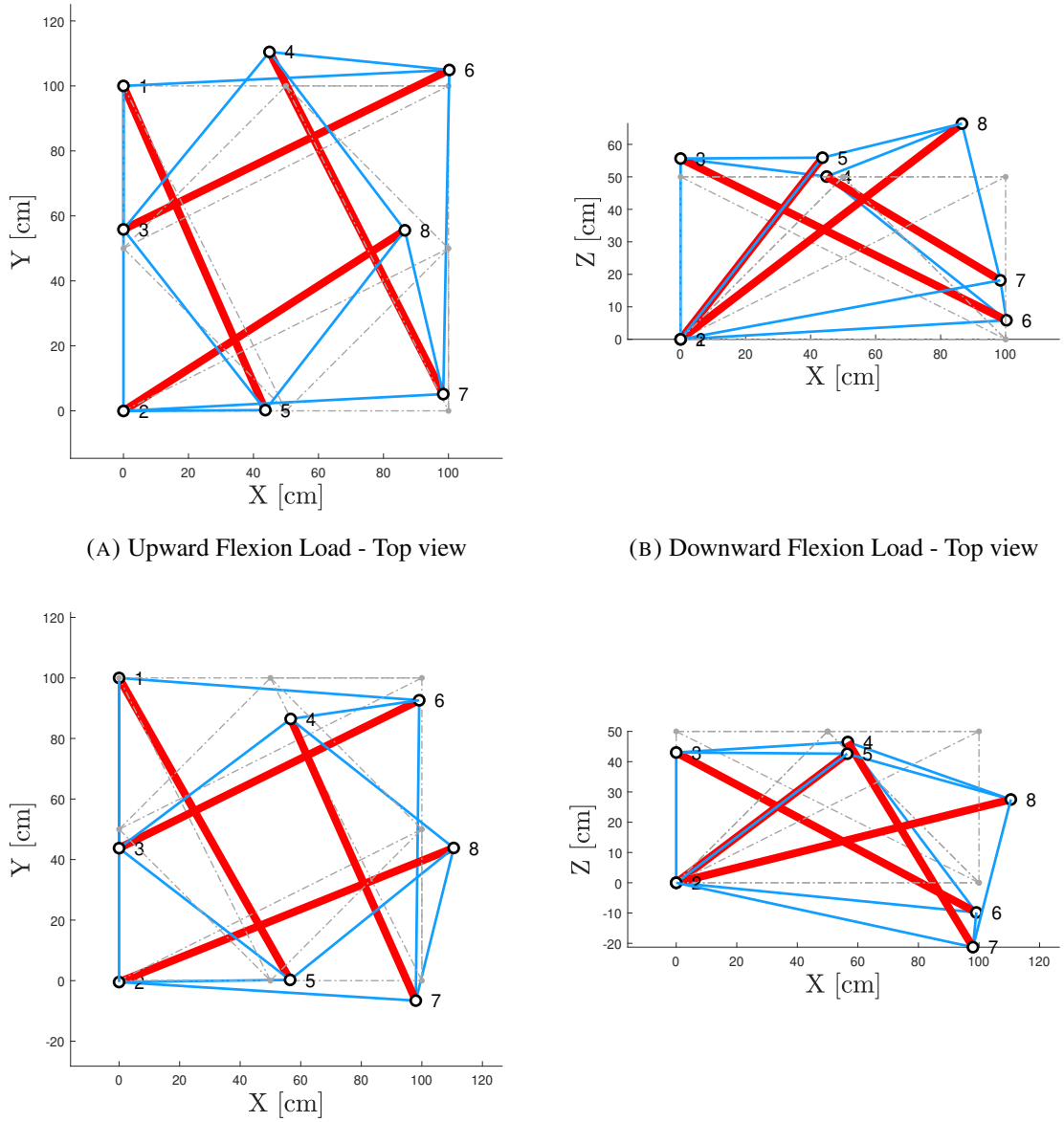

(A) Upward Flexion Load - Top view

(B) Downward Flexion Load - Top view

(C) Upward Flexion Load - Lateral

(D) Downward Flexion Load - Lateral

FIGURE 3.9: Top and lateral views of the deformed structure under up-downward flexion loads.

Regarding the internal stress evolution of each element against upward flexion load, the struts get more compressed as the cables increase their internal tension. This matches with the observations made in the behavior in traction Fig. 3.10. However, for the case of downward flexion load, cables number 1 and 4 experience a fall in tension of about a 12% and a loss in compression of 15% in bar number 13. The stress in the bar number 13 is stabilized for external loads higher than $2,5\ kN$ while bar number 14 is compressed about a 60% of its initial value for a load of $6\ kN$. For the rest of struts in this case a similar and quick evolution of the internal stress takes place (bars 15 and 16)

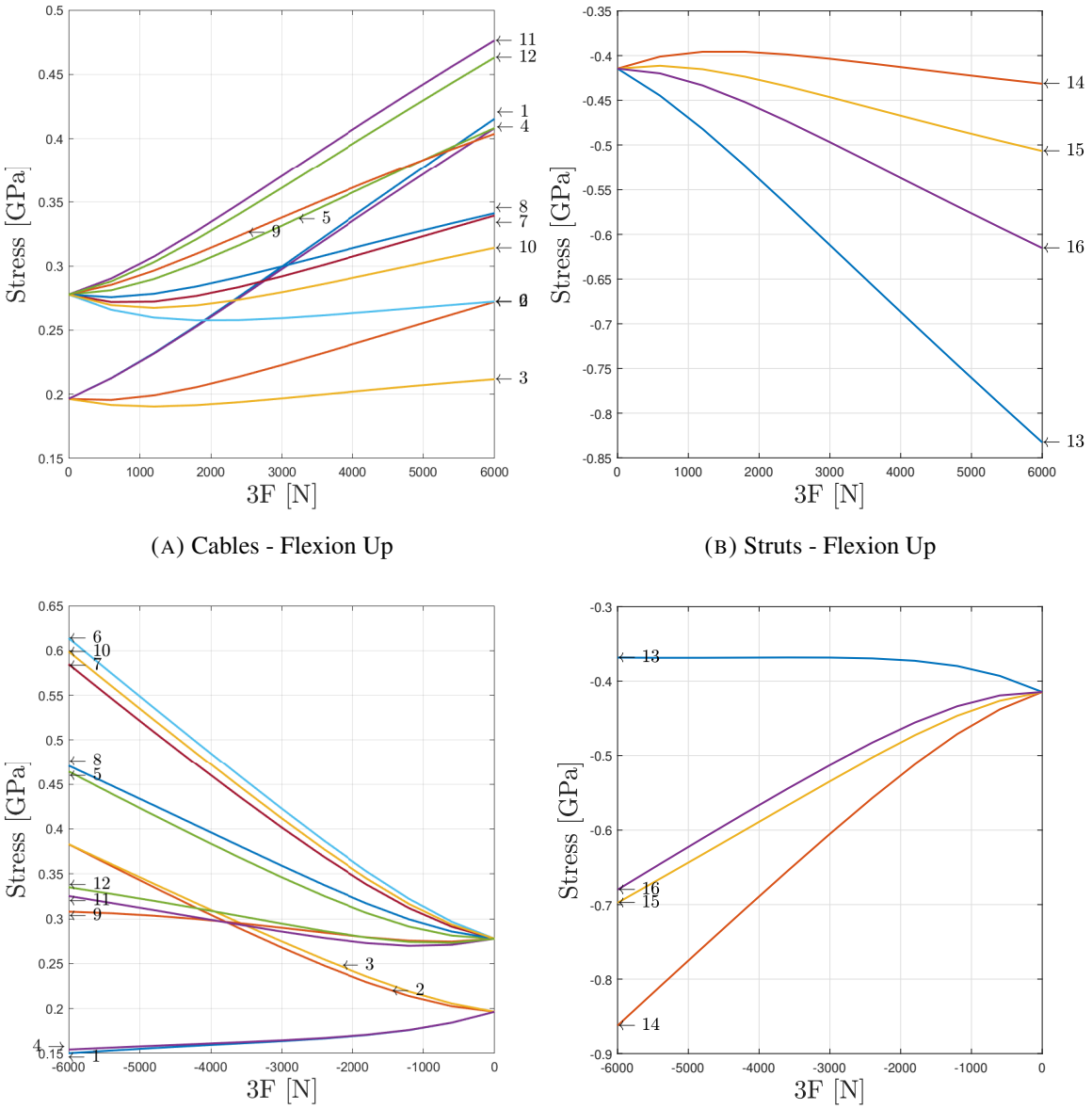

(A) Cables - Flexion Up

(B) Struts - Flexion Up

(C) Cables - Flexion Down

(D) Struts - Flexion Down

FIGURE 3.10: Evolution of the internal stress in members under upward and downward flexion loads.

The obtained results for traction, compression and flexion loads have been compared with the results obtained by Kebiche in [12]. The results show the same results as the obtained ones. it is concluded then that the developed code is correct and then it can be used for any tensegrity structure where nodal coordinates and connectivities as along as the material type.

3.3.2 The effect of pre-stress

In this section, the effect of prestressing a structure is presented. The aim is to show the advantages or drawbacks of a prestressed structure. To do so, both linear and non-linear algorithms have been implemented. The linear method does not need any iterative process while the non-linear one does (Newton Raphson). Considering the structure studied for the

program validation and considering traction forces, the displacements in both cases are as follows:

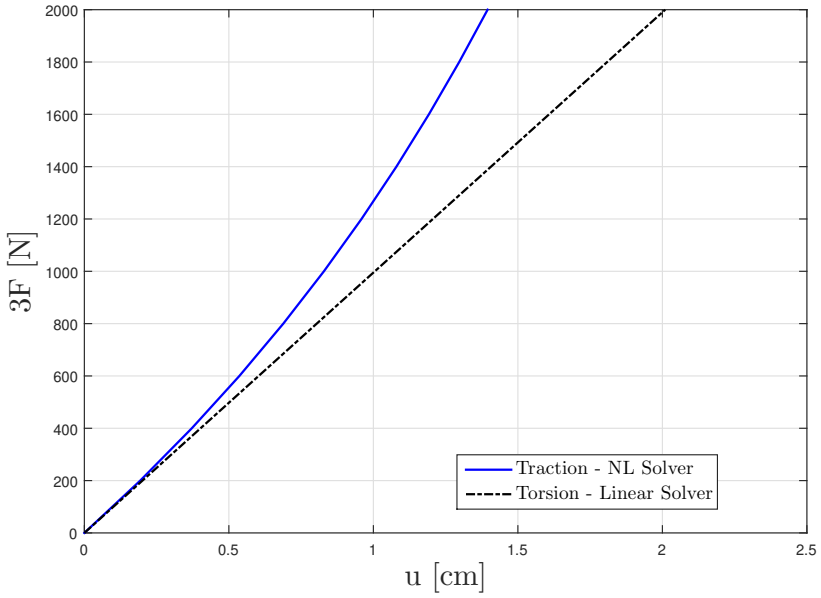

FIGURE 3.11: Difference between the solutions on displacements for Linear and non-linear Finite Element Methods

As it can be seen from Fig. 3.11, the structure has been notably improved with the non-linear method. With it, the structure is stiffened for a given load as to ensure that the internal forces and this external load become zero as much as possible. However, when a linear method is used, the structure responds to the applied load but only considering the initial level of pre-stress.

As the external load increases, the increment of displacements is reduced for the non-linear method while they become bigger and bigger for the linear method.

Chapter 4

Two Stage tensegrity Masts

In this chapter, the static analysis is presented for two stage tensegrity masts. The masts studied here have been defined by Skelton in [27]. A two stage tensegrity mast is composed by two tensegrity simplex as explained before.

For the numerical form-finding method the obtained masts had no aesthetics value and in some cases they went in a 2D solution. This masts are defined using the Reduced Coordinates Form-finding method and the Force-finding to define an initial state of sel-stress.

Once the initial self-stress design is found, the non-linear method explained in previous Chapters can be used to determine the behavior of the structure under external loads.

4.1 Form-Finding of Tensegrity Masts

The method of Reduced Coordinates, exaplined in Chapter 1 for the determination of a tensegrity structure, is applied to determine the initial shape of a tensegrity structure.

This method is used to determine the equilibrium-state of a two stage tensegrity mast with symmetrical relationship and known shape. Sultan and Skelton [28, 26], apply this method to a simple two stage tensegrity mast shown in Fig. 4.1. The mast consists of three struts per stage, held in place by three sets of cables - saddle, vertical and diagonal cables - between two rigid triangular plates (cables) at the top and bottom. The stages are basically two 3-strut tensegrity prisms one over another as we have previously seen in the numerical form-finding.

For this form-finding, the initial step is to determine a set of generalized coordinates which describe its configuration. For the two stage mast studied by Sultan, the 18 coordinates selected are:

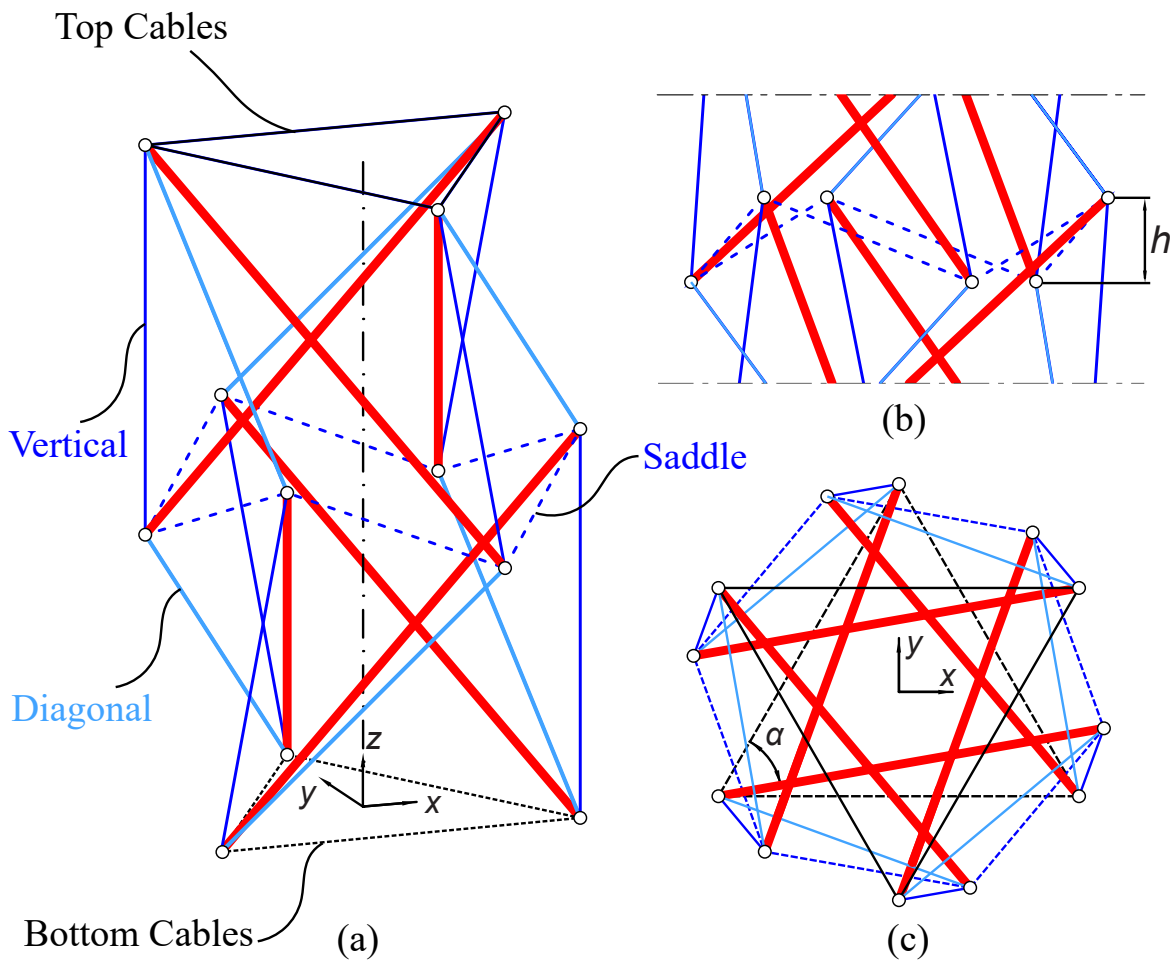

FIGURE 4.1: Sultan and Skelton's two stage tensegrity tower: (a) leteral view, (b) side view to better see the overlap and (c) top view.

- for each strut the azimuth angle is defined $_j$ (the angle between the vertical plane containing the strut and the $x-z$ plane), and the colatitude δ_j (angle between strut and z-axis). Also is noticeable the overlap h between both stages.
- Three rotations and three translation parameters defining the position and orientation of the top triangle of cables with respect the bottom one.

By the use of symbolic manipulation software(Maple, MuPAD, Mathematica, Matlab,etc), the length of each cable can be expressed in terms of the defined 18 coordinates and then differentitated to get an 18×18 matrix A, in symbolic form. At this point, the structure shape is still unknown and the existence of a self-equilibrated configuration depends on finding a suitable set of strut length. Sultan reduces the number of independent generalized coordinates by considering only symmetric configuration (same azimuth p_{s0}, colatitude δ). If a spatial symmetry in t is considered, the problem could be reduced to a 3×3 with the forces in the diagonal, saddle and vertical cables remain as the only unknowns. The equilibrium matrix A is finally defined as:

$$\mathbf{A} = \begin{bmatrix} \frac{\partial S}{\partial \alpha} & \frac{\partial V}{\partial \alpha} & \frac{\partial D}{\partial \alpha} \\ \frac{\partial S}{\partial \delta} & \frac{\partial V}{\partial \delta} & \frac{\partial D}{\partial \delta} \\ \frac{\partial S}{\partial h} & \frac{\partial V}{\partial h} & \frac{\partial D}{\partial h} \end{bmatrix} \tag{4.1}$$

where S, V and D are the length of the saddle, vertical and diagonal cables respectively. The expression for the length of this cables are derived analytically by Sultan as:

$$\begin{aligned} S &= \sqrt{h^2 + \frac{b^2}{3} + l^2\sin^2(\delta) - \frac{2}{\sqrt{3}}lb\sin(\delta)\cos\left(\alpha - \frac{\pi}{6}\right)} \\ V &= \sqrt{l^2 + b^2 - 2lb\sin(\delta)\sin\left(\alpha + \frac{\pi}{6}\right)} \\ D &= \sqrt{l^2 + \frac{b^2}{3} + h^2 - 2lh\cos(\delta) - \frac{2}{\sqrt{3}}lb\sin(\delta)\sin(\alpha)} \end{aligned} \tag{4.2}$$

where l is the length of the struts and b the length of the top and bottom cables (side length of the triangles). Due to the symmetry in configuration, this cables have the same length for both top and bottom stages (the saddle cables are common to the structure). The prestability condition is given by:

$$\mathbf{A}(\alpha, \delta, h)\mathbf{t} = \mathbf{0} \tag{4.3}$$

where t is the normalized internal force vector for saddle, vertical and diagonal cables. The non-trivial solution is then

$$\det(\mathbf{A}(\alpha, \delta, h)) = 0 \tag{4.4}$$

The solution of this quadratic equation is solved for the overlap analytically by Sultan, yielding:

$$h = \begin{cases} \frac{\cos(\delta)}{2\sin(\delta)\cos(\alpha+\pi/6)}\left(\frac{-b}{\sqrt{3}} + l\sin(\delta)\cos(\alpha+\pi/6) + \sqrt{\frac{b^2}{3} - 3p^2}\right) & \text{if } \alpha \neq \frac{\pi}{3} \\ \frac{l\cos(\delta)}{2} & \text{if } \alpha = \frac{\pi}{3} \end{cases} \tag{4.5}$$

For a given length of the top cables (b) and length of bars (l, can be also interpreted as the height of one stage), the overlap h can be evaluated and the adequate solution (of two possibles) is selected. With this, the nodal coordinates of the structure can be finally determined. For a two stage 3-strut tensegrity mast, the nodal coordinates are expressed as:

Stage	Plane	Node	x-coord	y-coord	z-coord
1	Bottom	1	r_b	0	0
		2	$r_b\cos(\gamma)$	$r_b\cos(\delta)$	0
		3	$r_b\cos(2\delta)$	$r_b\sin(2\delta)$	0
	Top Intersection	4	$x_1 + l_b\cos(\alpha_1)\sin(\delta)$	$y_1 + l_b\sin(\alpha_1)\sin(\delta)$	$l_b\cos(\delta)$
		5	$x_2 + l_b\cos(\alpha_1+\gamma)\sin(\delta)$	$y_2 + l_b\sin(\alpha_1+\gamma)\sin(\delta)$	$l_b\cos(\delta)$
		6	$x_3 + l_b\cos(\alpha_1+\gamma)\sin(\delta)$	$y_3 + l_b\sin(\alpha_1+\gamma)\sin(\delta)$	$l_b\cos(\delta)$
2	Top	10	$x_4 + l_b\cos(\alpha_1+\gamma/2)\sin(\delta)$	$x_4 + l_b\sin(\alpha_1+\gamma/2)\sin(\delta)$	$2l_b\cos(\delta) - h$
		11	$x_5 + l_b\cos(\alpha_1+\gamma+\gamma/2)\sin(\delta)$	$x_5 + l_b\sin(\alpha_1+\gamma+\gamma/2)\sin(\delta)$	$2l_b\cos(\delta) - h$
		12	$x_6 + l_b\cos(\alpha_1+2\gamma+\gamma/2)\sin(\delta)$	$x_6 + l_b\sin(\alpha_1+2\gamma+\gamma/2)\sin(\delta)$	$2l_b\cos(\delta) - h$
	Lower Intersection	7	$r_b\cos(\gamma/2)$	$r_b\sin(\gamma/2)$	$l_b\cos(\delta) - h$
		8	$r_b\cos(2\gamma+\gamma)$	$r_b\sin(2\gamma+\gamma)$	$l_b\cos(\delta) - h$
		9	$r_b\cos(2\gamma+2\gamma)$	$r_b\sin(2\gamma+2\gamma)$	$l_b\cos(\delta) - h$

TABLE 4.1: Nodal coordinates for a three-strut two stage tensegrity mast

where r_b is the base radius of the top and bottom triangles, l_b the length of the struts, α_1 is the azimuth angle of a bar connected to node 1 and another one (will be the same for all the bars), δ is the declination angle, h the overlap between stages and γ is $2\pi/3$ for this tensegrity. Note that this nodal locations are distributed in the xy plane of a circle and located on four different levels. For this case, the structure has 6 bars and 24 cables (6 vertical, 6 diagonal and 6 saddle ones).

The two stages are formed by two simplex tensgrity units composed by 3 struts each. the 3 bars forming a tensegrity unit are rotated either in clockwise or in anticlockwise direction. The top strings connecting the top nodes of each bar support the nect stage where the struts are rotated in an opposite direction to the previous stage. Following this explanation and Tab. (4.1) it is possible to construct as many stages as desired.

Note that this method requires some nodal coordinates witch are set in symbolic form to find a solution for the desired l_b and r_b for an overlap that fulfills the self-stress equilibrium condition Eq. (4.3). The connectivities for this type of structure can still be done manually due to the small number of elements.

The steps to determine the solution for the overlap is the following:

1. Generate the nodal connectivity and type of material data. The connectivities are sorted by symmetry groups. The first 6 elements correspond to the top and bottom cables (blue), the next 6 correspond to the vertical cables(cyan), followed by 6 saddle cable elements (dashed-blue), 6 diagonal cables and finally 6 bars (red).

2. Set the nodal coordinates as specified in Tab. (4.1) as a function of symbolic variables α, δ, . The length of the of the bars l_b and the radius of the top and bottom triangles r_b are design variables.

3. The length of the saddle vertical and diagonal cables are determined as long as the length of each element. Then, the partial derivatives in Eq. (4.1) are computed to determine the equilibrium matrix A.

4. The prestressability condition is that the determinant of the equilibrium matrix must be equal to zero. Using Matlab *solve* function for the overlap h, two solution are obtained as a function of α and δ. This two parameters can be now set as design variables to and play with the shape of the tensegrity. This two angles are used by Skelton to deploy this two stage mast as it will be seen.

5. Evaluating for the correct solution of the overlap h (non-negative one), the nodal coordinates are finally obtained and the initial self-stress design can be done.

The shape of the studied structure has an azimuth angle α of 200° and a declination angle δ of 60° (they have been selected as suitable angles proposed by Skelton). The top and bottom triangles have a radius of 50 *cm* and the bars a length of 100 *cm*. The following structure shows the geometry of the structure to be analyzed.

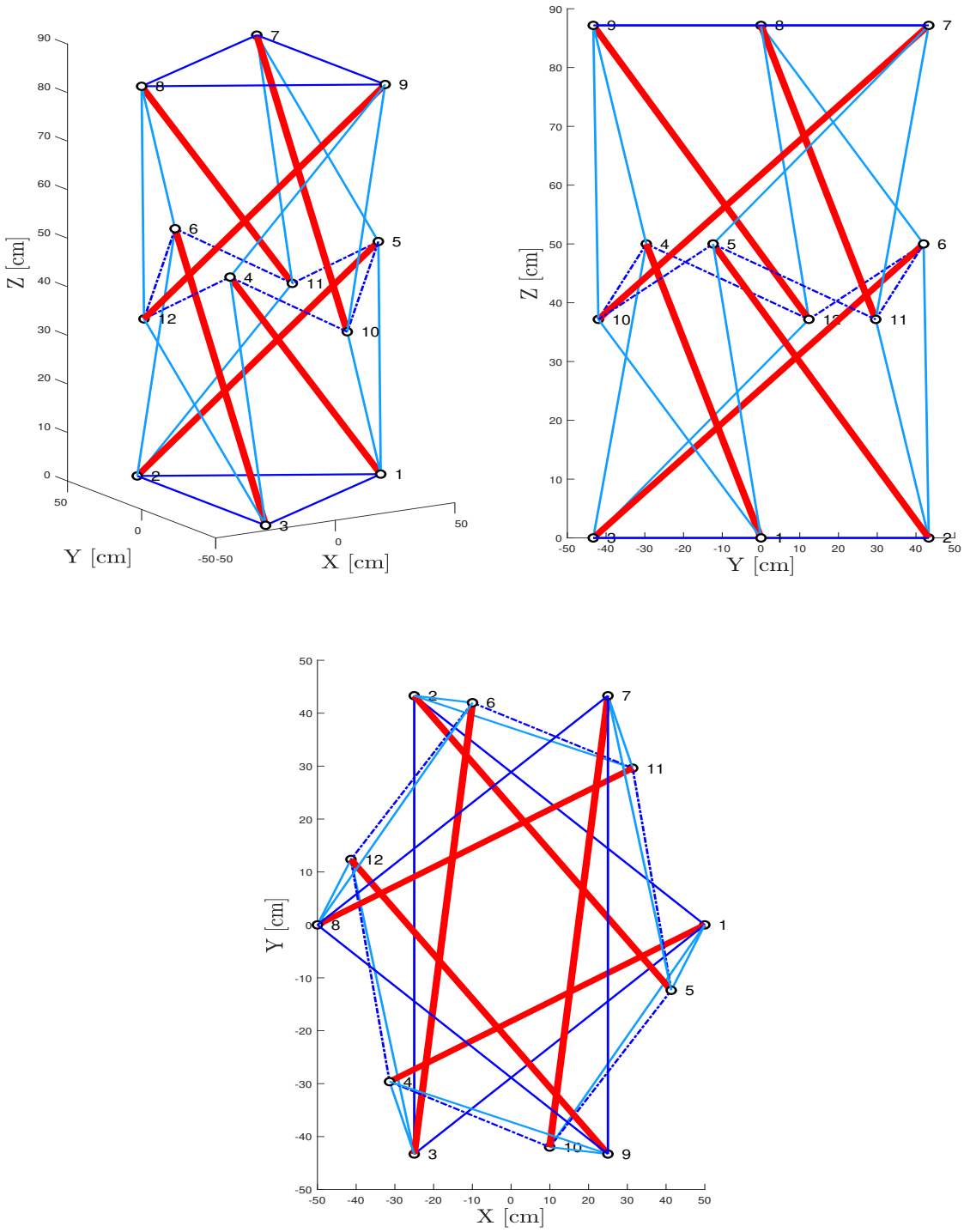

FIGURE 4.2: Side and Top view of a the deformed tensegrity mast under compression loads.

the nodal coordinates of the structure obtained in the previous procedure is shown in the following table,

Node	x	y	z
1	50.0000	0	0
2	-25.0000	43.3013	0
3	-25.0000	-43.3013	0
4	-31.3798	-29.6198	50.0000
5	41.3414	-12.3658	50.0000
6	-9.9616	41.9856	50.0000
7	25.0000	43.3013	87.1697
8	-50.0000	0.0000	87.1697
9	25.0000	-43.3013	87.1697
10	9.9616	-41.9856	37.1697
11	31.3798	29.6198	37.1697
12	-41.3414	12.3658	37.1697

TABLE 4.2: Noda coordinates

4.2 Stiffness Under external loads

As the nodal coordinates and the connectivities are known, the initial self stress design can be carried out as explained in section. For the designed structure only 1 state of self-stress exists ($s = 1$). This allows to determine the normalized pre-stress coefficients q for each group of symmetry which are:

Element	Pre-stress coeff.
Top and Bottom cables	1.000
Vertical Cables	1.659
Saddle Cables	4.154
Diagonal Cables	1.434
Struts	-2.725

TABLE 4.3: Prestress coefficient for each group of symmetry obtained from the initial self-stress design.

Where obviously, the bars are in compression are in compression and all the cables in tension, being the saddle cables the ones carrying more pre-stress.

Following the procedure as in Chapter 4 for the stiffness analysis of a 4-strut tensegrity prism, the analysis under external loads for this type if structure is made by considering 4 types of load: compression and traction, bending in two directions. The loads will be applied at the top surface of the upper stage (nodes 7, 8 and 9). Fig. 4.3 shows the different loads that will be studied. The applied force F is considered to be 2 kN over each node. The pre-stress coefficient p_{s0} is considered to be 100 N/m and the Young Modulus and cross-sections areas of 4 GPa and 2.8 cm^2 for cables and 20 GPa, 0.325 cm^2 for struts.

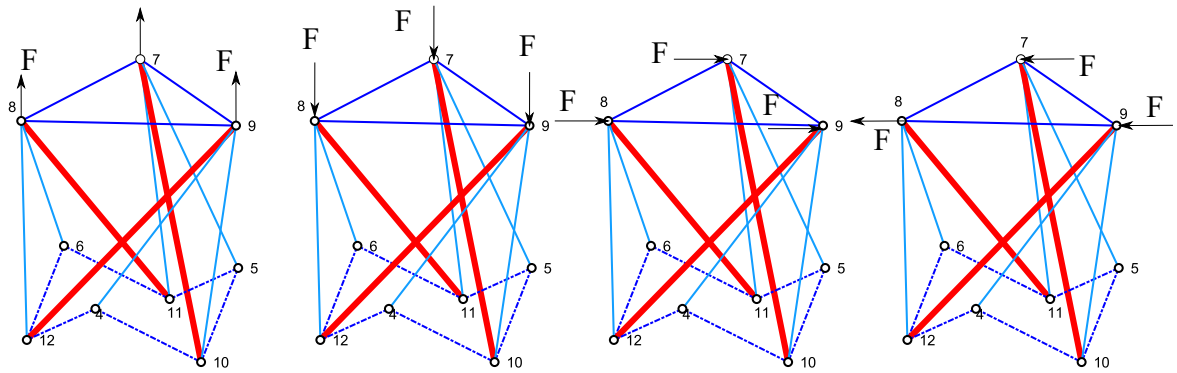

FIGURE 4.3: Different Loads from lefto to right: Compression ($-z$), traction and bending in direction B1 (y) and B2 ($-y$) (c) [30]

The structure responds differently to compression and traction again, due to its nonlinear nature. However, the anisotropic behavior here is not notorious as in the example studied in Chapter 3. When the structure is tractioned or compressed, it becomes stiffer as the external loads increase. This is because the level of pre-stress forces is changing (increasing) at each iteration for each external load, which affects the geometric stiffness matrix. Then, as The structure responds quite better to tractional loads as for an applied force of 2 *kN*, the displacements in traction are about 14 *cm* while for compression they are 20 *cm*.

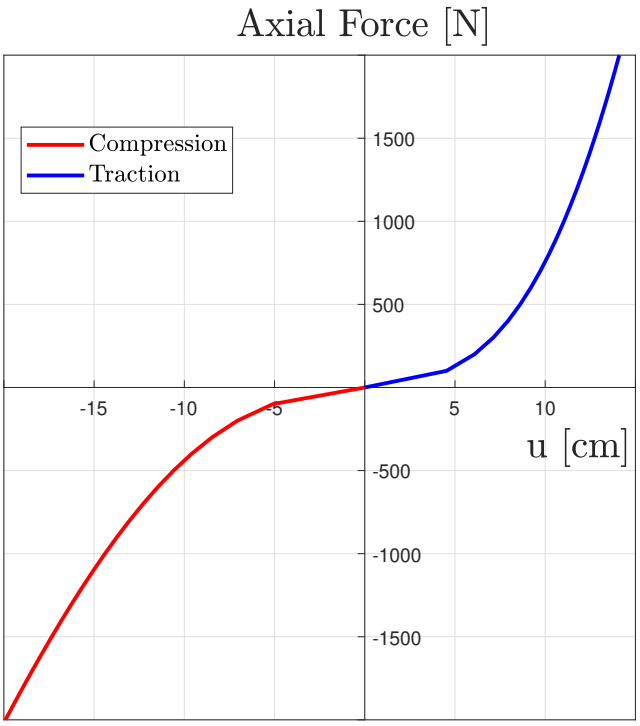

FIGURE 4.4: Average displacements of nodes 7,8 and 9 in the z direction for different traction and compression loads.

To better see the shape of the structure under the given external load, the deformed and initial structures are presented in the following plots:

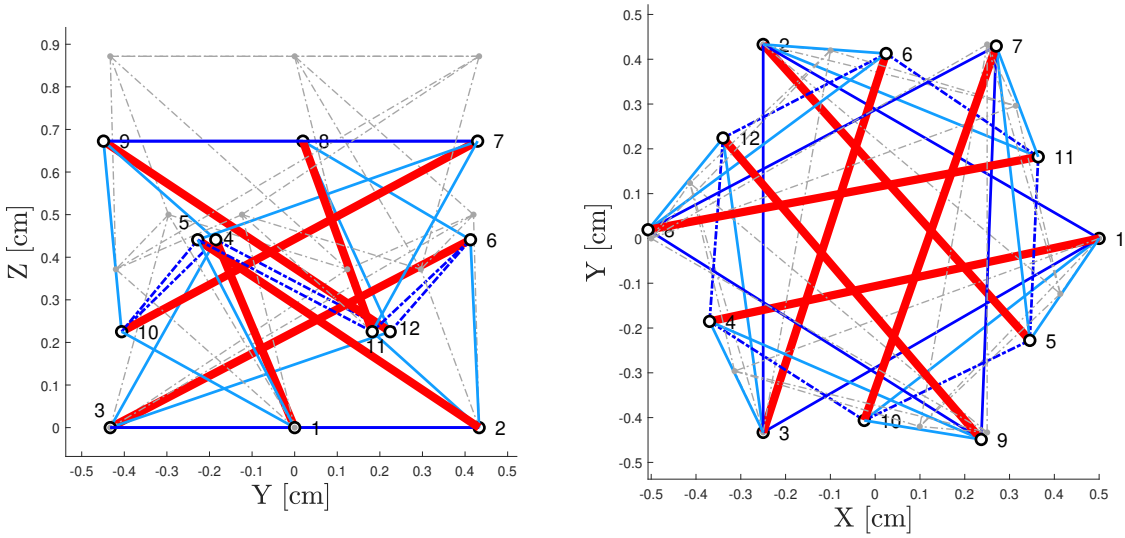

FIGURE 4.5: Side and Top view of a the deformed tensegrity mast under compression loads.

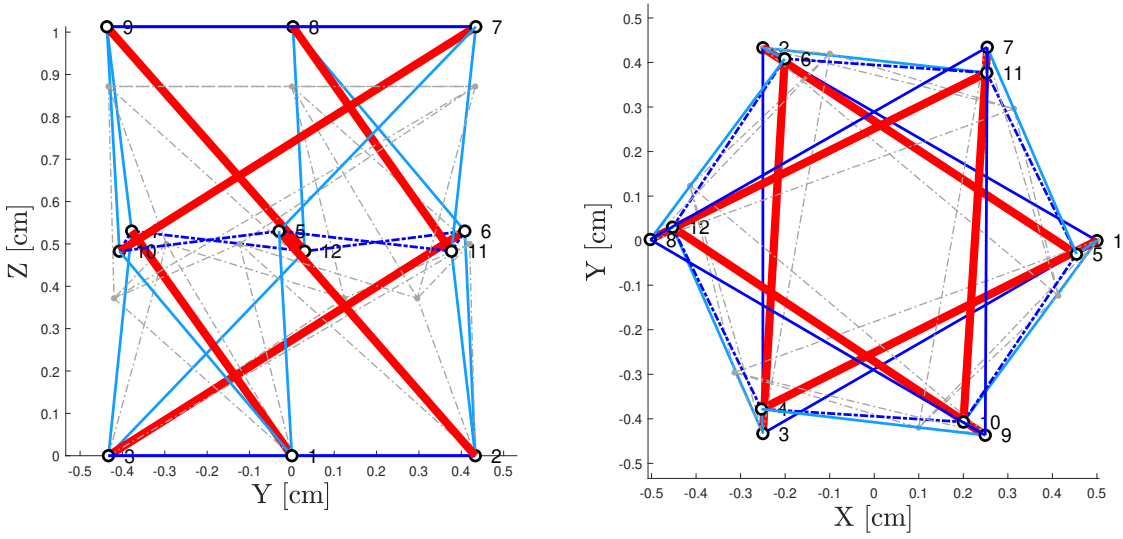

FIGURE 4.6: Side and Top view of a the deformed tensegrity mast under Traction loads.

If bending loads are considered, it is noticed that the structure displacements will increase in both direction as the applied load increases. For the case of bending in the negative direction of y (B1), the stiffness of the structure is constant until one or more cables go slack. When this occurs, the bending stiffness starts decreasing non-linearly for the applied loading. This fat can be solved in both cases by changing the pre-stress level p_{s0}.

For different levels of initial pre-stress p_{s0}, the structure seems to be stiffer. This can be seen for all the types of load but in a biggest ratio for the traction loads. Fig. 4.10 shows that as the pre-stress level p_{s0} is increased, the displacements become smaller for the same applied load. This is because the cables come more tensioned and as a consequence, the structure improves its stiffness. However, if this initial pre-stress value is too small

(i.e. $p_{s0} = 55N/m$), the cables on the structure become slack and then the stiffness of the structure is lost. The cables in this case become slack (get compressed, which is not feasible) when an external load of 30 is applied at each node.

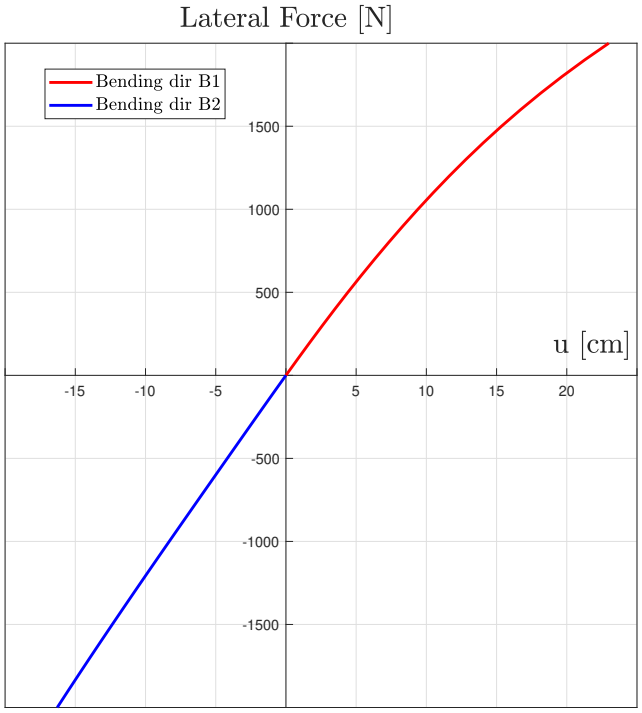

FIGURE 4.7: Average displacements of nodes 7,8 and 9 in the y direction for different bending loads loads.

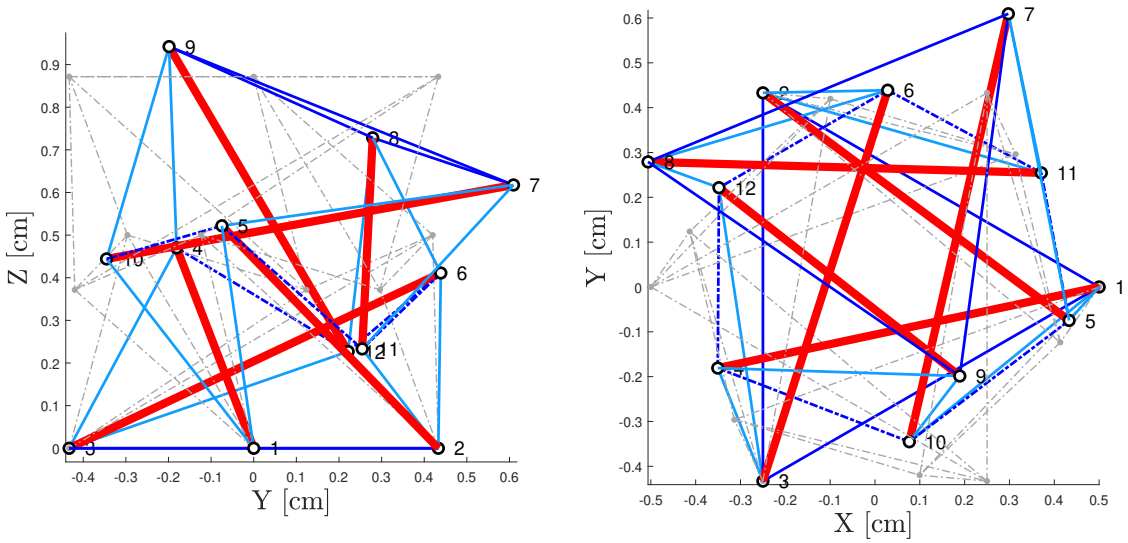

FIGURE 4.8: Side and Top view of a the deformed tensegrity mast under Bending loads.

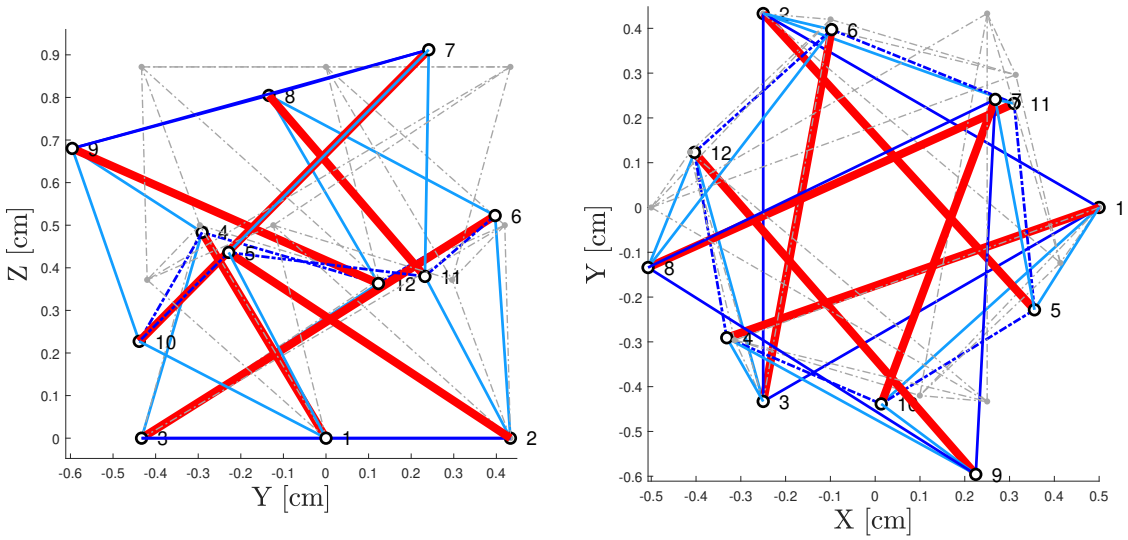

FIGURE 4.9: Side and Top view of a the deformed tensegrity mast under Bending loads in direction B1.

Considering now different values for the initial pre-stress level, which is a design parameter. The average displacements on the upper surface for different initial levels-of pre-stress in the four direction of loading application are shown in the following figures:

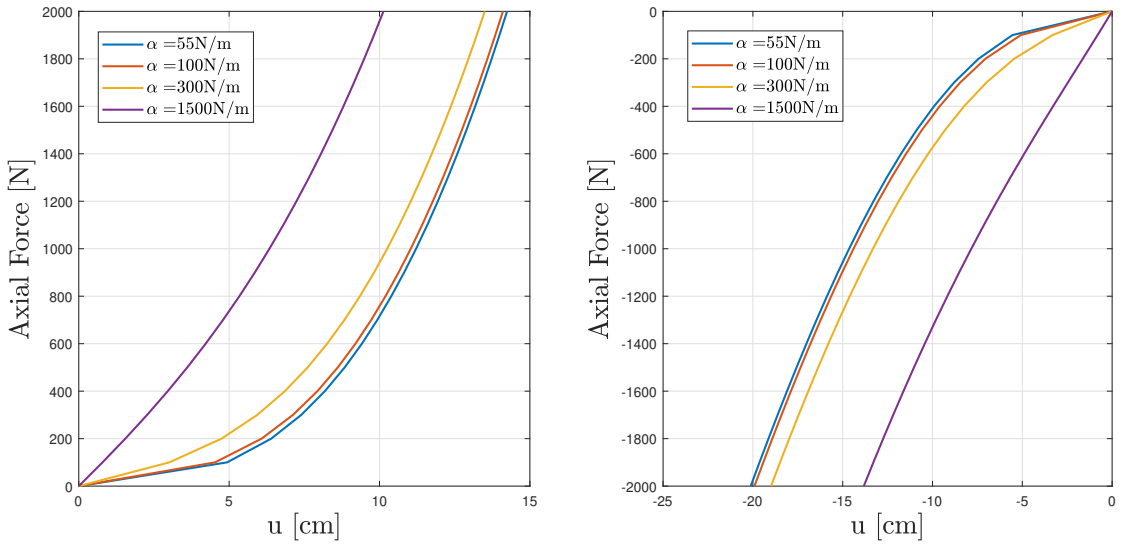

FIGURE 4.10: Average displacements of nodes 7,8 and 9 for different levels of pre-stress and compression-traction loads in direction B2.

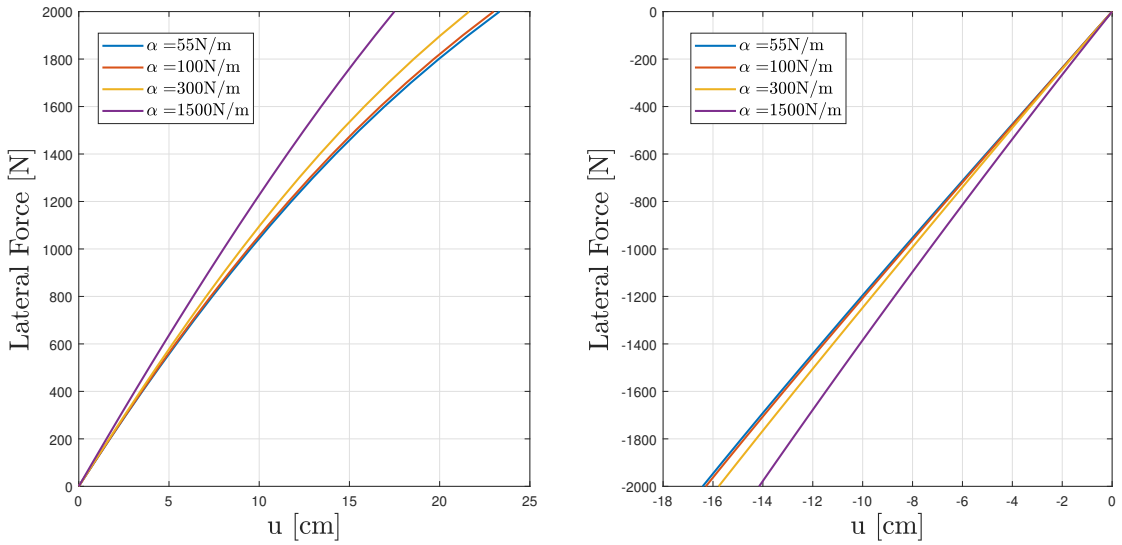

FIGURE 4.11: Average displacements of nodes 7,8 and 9 for different levels of pre-stress and bending loads loads.

It is noticeable that the stiffness of the structure is improved as the initial pre-stress level p_{s0} is increased. And it does in a notorious manner for the case of Axial forces (compression and traction). The problem for the bending stiffness has been solved with less effect.

4.2.1 Control and Deployment

Tensegrity structures are perfect candidates to be actively controlled structures as the control system can be directly embedded in the structure. That is, for example, use the tendons or cables as actuators and/or sensors. To control of a tensegrity structure can be done by forcing the structure to move along the equilibrium maniform. The equilibrium manifold for this mast is determined by evaluating positive solutions for the overlap by setting different azimuth α and declination δ angles, as made by Skelton [26]. With this an equilibrium surface can be drawn where the path fulfilling the condition of equilibrium is determined.

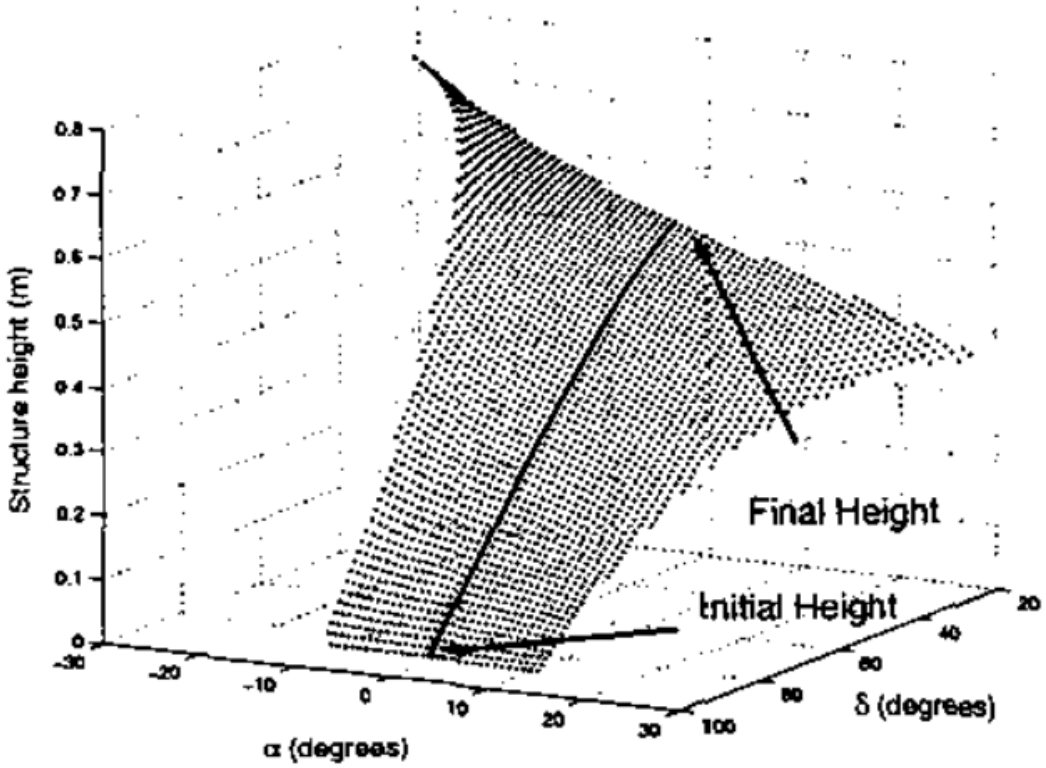

FIGURE 4.12: Equilibrium surface for a two stage tensegrity mast considering $r_b = 0.27\ m$ and $l_b = 0.4\ m$. Results given by Skelton [26]

In this section, the deployment of this type of mast is described. From the reduced coordinates method, it is easy to implement the previous mentioned equilibrium surface and the deployment can be idealized a time varying function for the declination angle δ, for example, $\delta(t) = 90° - 63°t$. For each declination angle, the initial-self stress design can be applied to determine the force carried by each member. Skelton have had determined that the top and bottom cables, as long as the struts will maintain a constant length if the deployment path determined in the equilibrium surface is followed. However, the vertical cables become bigger while saddle and diagonal cables decrease in length.

The results for this part where not computed due to lack of time for the delivery. however, the following figure shows the deployment process studied by Skelton in [26]

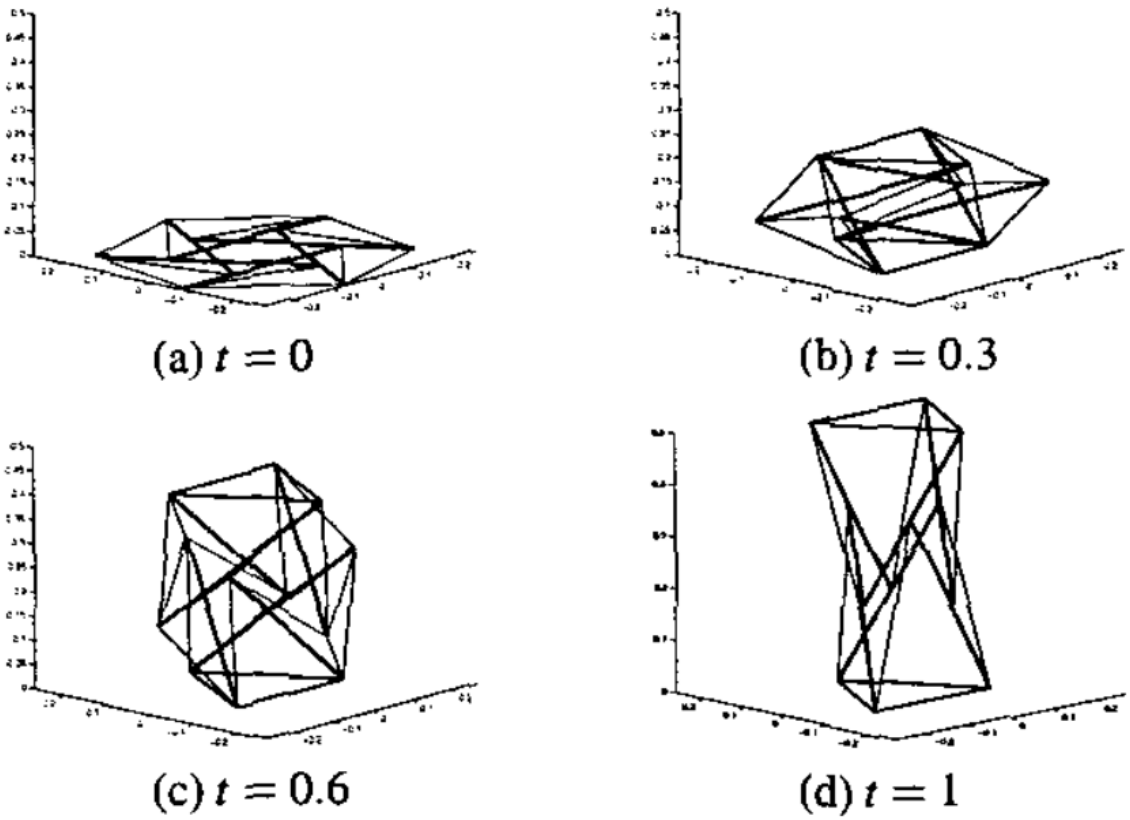

FIGURE 4.13: Deployment process for the sequence line shown in Fig. 4.12 [26]

Chapter 5

Conclusions

5.1 Analysis Methods

On of the principals aims of this Final Master Thesis was to determine and provide various methods for the form-finding of tensegrity structures. It was seen that there are various types of methods organized in static and kinematic groups. In this project, static methods have been used, which objective is to find an equilibrium configuration that allows the existence of a state of self-stress. In general, the static methods seem to possess more usable features than the kinematic ones.

It has been seen that if the aim of a researcher is to determine new shapes and configuration topology, the force-density method developed by Schek is well suited for this purpose. A numerical force-density method has been developed to determine 3-D tensegrity structures by just an idea of how the cables and struts are connected and a prototype force-density vector. However, it presents some difficulties while dealing with structural members length, symmetry, aesthetics and geometry orientation. This is due to the variation in the force-density vectors, which does not respect unilateral behavior between elements (bars an cables).

The reduced coordinates form finding method is useful for situations where more information about the structure geometry is known. This method has been implemented to solve a two stage cylindrical tensegrity mast where the nodal coordinates can be expressed as two tensegrity simplex rotated certain angle and with and overlap between stages. Against the numerical force-density method, the length of the elements can be controlled and then, the symmetry of the structure.

Finally, it is concluded that there are different types of form-finding methods for tensegrities but each one has a function and then, anyone is suitable for general applications.

5.2 Pre-Stressed Structures

Another aim of this project was to determine how better can be a pre-stressed structure against conventional pin-jointed structures. This has been done through the analysis of a pure tensegrity structure against external loads. To determine the response to external loads, two Finite Element Methods have been implemented. For both cases, an initial self-stress state is determined and the internal force vector is then computed for an initial level of

pre-stress. In the first method, called linear FEM with small displacements assumption, the internal force-vector is constant and equal to the one defined in the initial self-stress design. For the second method, a non-linear variation of FEM considering geometrical stiffness due to pre-stress, the internal force vector is changed so as to ensure equilibrium at each node. This latter then becomes iterative and is solves by using Newthon Raphson method.

The previous analysis shows that the structural behavior is notable different. For the linear method, the displacements increase as long as the external force increases. This produces slack of the cables as they start to take compressing values (which is not feasible) and then, a larger deformation of the structure occurs. The second method showed that a consciously pre-stressed structure becomes stiffer as external loads are increased.

5.3 Uses In Space Industry

The wide range of possibilities for geometrical design, lightness, material saving and great resistance and deployability that this structures offer, make them an interesting topic of study in the field of space applications. Actually, volume saving on carried payloads for space missions are crucial if large structures are transported. Deployable structures have been used for many years in space applications such as, antennas, solar array or masts. Some types of masts are similar to tensegrities as they are pre-stressed structures composed by bars and cables.

In this project, the simplest tensegrity mast with two stages have been studied. The objective was to determine how this mast will respond under external forces using the non-linear finite element analysis. The results show that they are really good under compression and traction loads but bad under bending. This lack on bending stiffness can be solved by changing the design parameters (Young Modulus, Cross-section, initial pre-stress force, etc). The deployability sequence for this mast has been discussed.

The inconvenient of this type of mast is that it does not reach full stiffness until the last stage has been completely deployed. This a huge limiting factor for the application of this type mast as during the deployment sequence the mast is very flexible. In a real scenario this can be solved by a central road that pushes the upper surface of the mast.

The above problem can be solved by using "false" tensegrity structures where struts are in contact (Class II tensegrities). This fact will, however, reduce the capabilities of the structure to be deployed. The trade-off then becomes between fast and easy deployment and compact packaging, or the stiffness and strength capabilities.

5.3.1 Future Work

One of the main focus for future research must be the applications of tensegrity structures. regarding their morphology, the number of possible configurations exceeds the possible applications, and then, only a few types of tensegrity is useful for real applications.

A general method for tensegrity structures regarding form-finding is necessary to be developed as actual methods are suitable for different tensegrity types. For a given study, one method must be select against others depending on the desired analysis.

Personally, the implemented methodology for a two stage mast must be implemented for an n-stage tensegrity mast. Due to lack of time, it has not been possible to dedicate all the time that was intended to this part, therefore it remains as personal future work.
Another important thing to solve is the lack of stiffness of the tensegrity structures in deployment as long as the bending stiffness under external loads (although it can be improved by setting the correct materials and structure, e.g - Skelton *et al*. [26] analyze planar tensegrity structures that are efficient in bending). As mentioned before, for deployable masts, the actual studies have shown that the mast is flexible until the last stage has been deployed. This, in fact, is not desired and it supposes a huge barrier to use tensegrities for this purpose.

Bibliography

[1] Musa Abdulkareem. *Tensegrity Structures: Form-finding, Modelling, Structural Analysis, Design and Control*. 2013.

[2] G. Gomez Estrada et all. "Numerical form-finding of tensegrity structures". In: *International Journal of Solids and Structures* (2006). DOI: doi:10.1016/j.ijsolstr.2006.02.012.

[3] C.R. Calladine. "Buckminster Fuller's "Tensegrity" structures and Clerk Maxwell's rules for the construction of stiff frames". In: *International Journal of Solids and Structures* (1978). Pages 161-172.

[4] William B Carlson, Dave Williams, and Robert E Newnham. "Piezotensegritic structures for transducer applications". In: *Materials Research Innovations* 3.3 (1999), pp. 175–178.

[5] R. Connelly. "Rigidity and energy. Inventiones Mathematicae". In: *Inventiones Mathematicae* (1982). 66(1), 11–33.

[6] Reg Connelly and Maria Terrell. "Globally rigid symmetric tensegrities". In: *Structural Topology 1995 núm 21* (1995).

[7] Wenru Dong. *Topology, Stability and Robustness of Tensegrity Structures*. Imperial College London, 2017.

[8] R Buckminister Fuller. "Tensile-integrity structures". In: *Patente US3063521, concedida* (1965).

[9] Buntara Sthenly Gan. *Computational Modeling of Tensegrity Structures*. Springer, 2020.

[10] Buntara Sthenly Gan. *Computational Modeling of Tensegrity Structures*. London: Springer, 2020. ISBN: 978-3-030-17835-2.

[11] A Hanaor. "Double-layer tensegrity grids as deployable structures". In: *International Journal of Space Structures* 8.1-2 (1993), pp. 135–143.

[12] K Kebiche, MN Kazi-Aoual, and R Motro. "Geometrical non-linear analysis of tensegrity systems". In: *Engineering structures* 21.9 (1999), pp. 864–876.

[13] Hassan A Khayyat. *Conceptual design and mechanisms for foldable pyramidal plated structures*. Cardiff University, 2008.

[14] Alan Shu Khen Kwan. "A pantographic deployable mast." PhD thesis. University of Cambridge, 1991.

[15] Haresh Lalvani. "Origins of tensegrity: views of Emmerich, Fuller and Snelson". In: *International Journal of Space Structures* 11.1-2 (1996), pp. 27–27.

[16] Manfred Leipold, H Runge, and C Sickinger. "Large SAR membrane antennas with lightweight deployable booms". In: *28th ESA Antenna Workshop on Space Antenna Systems and Technologies, ESA/ESTEC*. European Space and Technology Research Centre Noordwijk, The Netherlands. 2005, p. 8.

[17] Martin M Mikulas. "State-of-the-art and technology needs for large space structures". In: *ASME Monograph on Flight-Vehicle Materials, Structures, and Dynamics Technologies* (1993).

[18] Rene Motro. "Tensegrity systems: the state of the art". In: *International journal of space structures* 7.2 (1992), pp. 75–83.

[19] René Motro. *Tensegrity: structural systems for the future*. London: Kogan Page Science, 2003.

[20] Sergio Pellegrino. "Large retractable appendages in spacecraft". In: *Journal of Spacecraft and Rockets* 32.6 (1995), pp. 1006–1014.

[21] Sergio Pellegrino. "Structural computations with the singular value decomposition of the equilibrium matrix". In: *International Journal of Solids and Structures* 30.21 (1993), pp. 3025–3035.

[22] Sergio Pellegrino and Christopher Reuben Calladine. "Matrix analysis of statically and kinematically indeterminate frameworks". In: *International Journal of Solids and Structures* 22.4 (1986), pp. 409–428.

[23] H.-J. Schek. "The force density method for form finding and computation of general networks". In: *Computer Methods in Applied Mechanics and Engineering, 3(1), 115–134* (1974). DOI: doi:10.1016/0045-7825(74)90045-0.

[24] M Schenk. *Statically balanced tensegrity mechanisms. A literature review.* 2005.

[25] Mizuho Shibata, Fumio Saijyo, and Shinichi Hirai. "Crawling by body deformation of tensegrity structure robots". In: *2009 IEEE international conference on robotics and automation*. IEEE. 2009, pp. 4375–4380.

[26] RE Skelton et al. *An introduction to the mechanics of tensegrity structures, dynamics and control of aerospace systems, University of California*. 2002.

[27] Robert E Skelton and Mauricio C De Oliveira. *Tensegrity systems*. Vol. 1. Springer, 2009.

[28] C Sultan, M Corless, and R Skelton. "Reduced prestressability conditions for tensegrity structures". In: *40th Structures, Structural Dynamics, and Materials Conference and Exhibit*. 1999, p. 1478.

[29] A. Tibert and S. Pellegrino. "Review of form-finding methods for tensegrity structures". In: *International Journal of Solids and Structures* (2011). DOI: https://doi.org/10.1260/026635103322987940.

[30] Gunnar Tibert. *Deployable Tensegrity Structures for Space Applications*. Royal Institute of Technology, 2002.

[31] Hoang Chi Tran and Jaehong Lee. "Initial self-stress design of tensegrity grid structures". In: *Computers & structures* 88.9-10 (2010), pp. 558–566.

[32] Lee J Tran HC. "Self-stress design of tensegrity grid structures with exostresses". In: *International Journal of Solids and Structures* (2010). DOI: doi:10.1016/j.ijsolstr.2010.05.020.

[33] Nicolas Vassart and René Motro. "Multiparametered formfinding method: application to tensegrity systems". In: *International journal of space structures* 14.2 (1999), pp. 147–154.

[34] Kaan Yildiz. *Cable Actuated Tensegrity Structures for Deployable Space Booms with Enhanced Stiffness*. 2018. URL: https://etda.libraries.psu.edu/files/final_submissions/17325.